confirming that BRCA1 was able to form a complex with DBC1. To address the functional importance of the DBC1–BRCA1 interaction, *in vitro*-translated DBC1 in the presence of [^{35}S] methionine was incubated with GST and GST fusion BRCT. As clearly shown in Figure 1C, [^{35}S]-labelled DBC1 bound the GST-fused BRCT protein, consistent with the results from the immunoprecipitation assay. These data indicated that DBC1 directly interacted with the BRCT domain. To map the region of DBC1 that interacts with the BRCT domain, GST pull-down assays were performed to test for the interaction with GST–BRCT and fragments of *in vitro*-translated DBC1 (Figure 1D). The amino-terminal region of DBC1 including the NLS interacted with the BRCT domain. These findings indicate that the DBC1 amino terminus including the NLS and the BRCT domain are both necessary and sufficient for the interaction between DBC1 and BRCA1. We further confirmed the binding of the BRCT domain to the DBC1 amino terminus using mammalian two-hybrid assays. In this assay, the VP16-fused amino terminus of DBC1 containing the NLS (VP-DBC1 N) exhibited a prominent interaction with the BRCT domain, whereas DBC1 lacking the amino terminus (VP-DBC1 ΔN) showed no interaction, underscoring the results of immunoprecipitation and GST pull-down experiments (Figure 1E).

DBC1 and BRCA1 colocalise in intact and apoptotic cells

Immunohistochemical studies using human breast specimens showed nuclear staining of DBC1 in the duct and adipose tissue (Figures 2A and B, respectively). Most breast cancer cells exhibited nuclear staining (Figure 2C), but this nuclear staining of DBC1 was not observed in cancer cells with an enlarged nucleus (Figure 2D, arrows). As previously shown, during tumor necrosis factor-α-induced apoptosis, DBC1 is translocated to the cytoplasm with a loss of the amino terminus containing the NLS (Sundararajan *et al*, 2005), and the expression of BRCA1 is downregulated by caspase-3-mediated cleavage during UV-induced apoptosis (Zhan *et al*, 2002). The changes in cellular distribution of DBC1 and BRCA1 during apoptotic processes were examined comprehensively under a confocal microscope in MCF-7 cells treated by UV-mediated death signalling. Both DBC1 (Alexa Fluor 555-conjugated anti-rabbit IgG, red) and BRCA1 (Alexa Fluor 488-conjugated anti-mouse IgG, green) were abundantly expressed and colocalised in the nuclei of control cells (Figure 2E, 1–4). In contrast to healthy cells, both DBC1 and BRCA1 are translocated to the cytoplasm in cells showing apoptotic morphological changes (Figure 2E, 5–8). The degree of colocalisation signal was quantified in both control and apoptotic cells, and these data indicated that UV-mediated apoptosis signalling prompted the translocation of these proteins (Figure 2F).

DBC1 represses the transcriptional activation function of BRCT

The result that the BRCT domain interacts with DBC1 led us to examine the role of DBC1 in the transactivation function of GAL4-fused BRCT. Transient transfection assays were performed using a 17M8-AdMLP-luc luciferase reporter plasmid, carrying

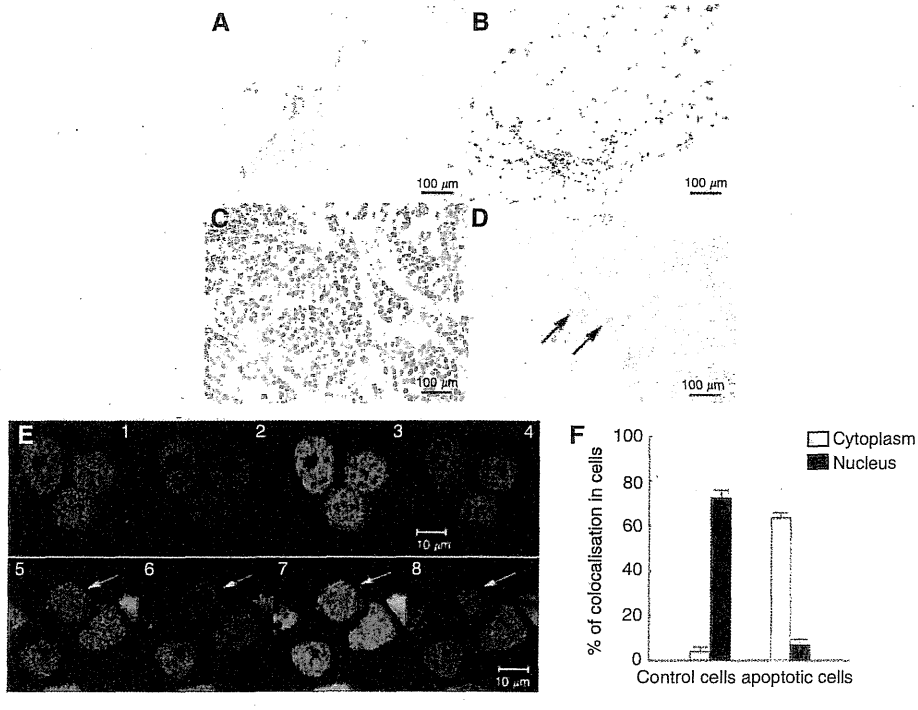

Figure 2 Immunohistochemical detection of DBC1 in human breast tissues and colocalisation of BRCA1 and DBC1 in MCF-7 human breast cancer cells. (**A**–**D**) Breast specimens were obtained at the time of diagnosis of breast cancer in accordance with the guidelines of the Ethical Board of Komagome Hospital. DBC1 showed nuclear staining of ductal epithelium (**A**) and adipose tissue (**B**) in breast specimens. DBC1 expression was observed in the nuclei of cancer tissues (**C**). Cancer cells exhibiting an enlarged nucleus showed a complete loss of DBC1 expression (**D**, arrow). (**E**) MCF-7 cells were either treated or not treated by ultraviolet (UV) light (0.24 J), fixed, and permeabilised. Cells were incubated with primary antibodies and subsequently with secondary antibodies. The expression of DBC1 (red) and BRCA1 (green) was investigated under confocal fluorescence microscopy (Carl-Zeiss). Representative immunofluorescence studies are shown (E, 1–4; control, 5–8; UV exposure for 10 min, E3 and E7; merge, E4 and E8; 4′,6-diamino-2-phenylindole staining). Arrows in E5–8 indicate a cell showing apoptotic morphological changes with the cytoplasmic expression of DBC1 and BRCA1. Bars indicate 10 μm. (**F**) The degree of colocalisation (BRCA1 and DBC1) was measured using a confocal microscope. The colocalisation signal was quantified in the nucleus and cytoplasm of cells separately.

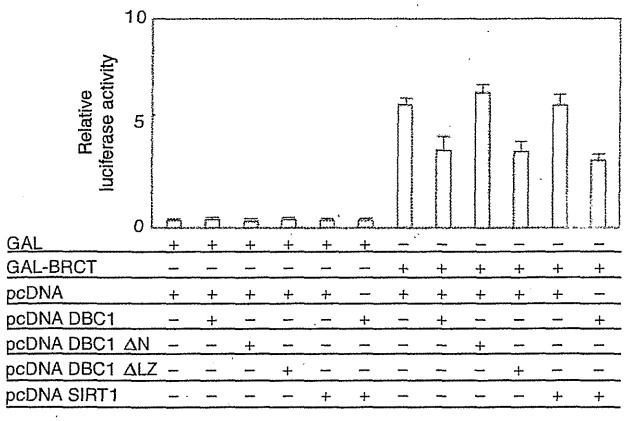

Figure 3 DBC1 represses transcription of GAL4–BRCT through its amino-terminal domain. Transient transfection assays were performed to examine the co-factor activity of DBC1 in the transactivation function of GAL4-fused BRCT. Cells (293T) were transfected with the indicated combinations of mammalian expression plasmids. At 24 h after transfection, the cells were harvested, and transfected whole-cell lysates were assayed for luciferase activity produced from the reporter plasmid (17M8-AdMLP-luc). DBC1 showed a specific repression of the transactivation function of BRCT. The amino terminus of DBC1 was indispensable for this inhibition of BRCT. SIRT1, a binding partner that has roles in cell senescence and tumourigenicity, had no effect on the transactivation function of BRCT. phRL *Renilla* CMV-luc vector was transfected as a control of transfection efficiency. Each experiment was repeated at least three times in triplicate. Error bars represent s.d.

eight tandem repeat GAL4 DNA binding sites (17M × 8) upstream of the major late promoter of adenovirus (AdMLP) driving the expression of the firefly luciferase gene. Although the GAL4–BRCT fusion protein (GAL–BRCT) activated the promoter activity of the reporter plasmid in 293T cells, the transcriptional activity of BRCT was significantly decreased by the expression of DBC1 in luciferase assays (Figure 3). DBC1 lacking an interaction domain with BRCA1 (DBC1 ΔN) lost its ability to inhibit the BRCT-mediated transactivation function (Figure 3). DBC1 lacking a binding region with SIRT1 deacetylase (DBC1 ΔLZ) suppressed the GAL–BRCT transactivation function. SIRT1 showed no influence on the GAL–BRCT transactivation function and on the repression of GAL–BRCT by DBC1. The BRCT-repression function of DBC1 was unaffected in the presence of resveratrol, a major activator of SIRT1, and trichostatin A, a histone deacetylase inhibitor (data not shown). These results suggest that the amino terminus of DBC1 has a significant role in the repression of GAL–BRCT and SIRT1 has no role in regulating the GAL–BRCT function.

DBC1 disrupts BRCA1-mediated SIRT1 expression

The previous chromatin immunoprecipitation assay showed that BRCA1 interacted with the SIRT1 promoter region between 1354 and 1902 and this binding resulted in an elevated expression of SIRT1 (Wang *et al*, 2008). We investigated whether DBC1 has an effect on the BRCA1-mediated stimulation of the SIRT1 promoter. An analysis of the effect of DBC1 on SIRT1-luciferase constructs containing various lengths of SIRT1 promoter regions upstream of the luciferase gene was performed and DBC1 demonstrated a specific downregulation of BRCA1-mediated stimulation on the SIRT1 promoter (SIRT1 1-2852 Luc), evidenced by the expression of DBC1 (Figure 4A). As expected, DBC1 ΔN showed no influence to inhibit the BRCA1-mediated transactivation function of SIRT1-luciferase reporter constructs, whereas DBC1 ΔLZ showed repression on the SIRT1-luciferase transactivation function mediated by BRCA1. We next examined the effect of siRNA-mediated depletion of DBC1 or BRCA1 on their downstream genes. As expected, knockdown of BRCA1 expression by BRCA1-specific siRNA completely abrogated the expression of SIRT1 (Figure 4B, lanes 4 and 5), validating the previous report that the expression of SIRT1 is indeed dependent on BRCA1 (Wang *et al*, 2008). As shown in Figure 4B, lanes 2 and 3, depletion of endogenous DBC1 increased the expression of SIRT1. To demonstrate that SIRT1 functions on the p53 acetylation level (Zhao *et al*, 2008), we tested whether depletion of BRCA1 or DBC1 indeed influences the expression of acetylated p53. Consistent with previous studies (Kim *et al*, 2008; Zhao *et al*, 2008), RNAi-mediated knockdown of DBC1 expression resulted in hypoacetylation of p53 (Figure 4B, lanes 2 and 3), whereas depletion of endogenous BRCA1 had no influence on the expression level of acetylated p53 (Figure 4B, lanes 4 and 5). Depletion of DBC1 resulted in a downregulation of p21, a transcriptional target of BRCA1 (Figure 4B, lanes 2 and 3). Thus, our data demonstrate that DBC1 has a critical role in regulating downstream gene expressions dependent on BRCA1 *in vivo* such as SIRT1 and p21. To test whether DBC1 and BRCA1 were indeed recruited to the SIRT1 promoter, we performed a chromatin immunoprecipitation assay using the SIRT1 gene promoter 1354–1902, a region known to recruit BRCA1 (Wang *et al*, 2008). As expected, a clear recruitment of endogenous BRCA1 to the target sequence (1354–1902) in the SIRT1 promoter was observed in HeLa cells (Figure 4C). Besides this BRCA1 recruitment, DBC1 and SIRT1 were also detected in the promoter region, presumably reflecting the complex formation of BRCA1-DBC1 on the SIRT1 promoter (Figure 4C).

DISCUSSION

The transcriptional activation function of BRCT is believed to be a key to its tumour-suppressor activity (Chapman and Verma, 1996; Monteiro *et al*, 1996). The importance of BRCT for transcriptional control and growth suppression is also highlighted by the fact that cancer-associated mutations attenuated both, but a neutral polymorphism did not (Humphrey *et al*, 1997; Yarden and Brody, 1999). BRCT possesses an autonomous folding unit defined by conserved clusters of hydrophobic amino acids, and BRCT is likely to represent a protein interaction surface (Saka *et al*, 1997). Although a number of proteins have been identified to interact with the BRCT domain, most of them activate the transcriptional function of BRCT (Wada *et al*, 2004; Oishi *et al*, 2006), and the repressors of BRCT have been poorly studied until now (Chen *et al*, 2001). Here, we clearly showed that endogenous DBC1 associated with BRCA1 *in vivo* and *in vitro*, which suggests the possibility that DBC1 might have a functional relationship with BRCA1-related phenotypical changes. This interaction between BRCA1 and DBC1 was physiologically functional because our results indicated that the DBC1-containing complex might modulate a role of BRCA1 in living cells, repressing BRCT function. In this respect, DBC1 seems to have a tumourigenic role in living cells. The BRCT domain is found in a diverse group of proteins implicated in DNA repair and cell-cycle checkpoint control (Bork *et al*, 1997; Callebaut and Mornon, 1997). A point mutation within the BRCT domain (A1708E) was shown to be critical for DNA damage response by treatment with DNA-damaging agent methylmethane sulphonate (Zhong *et al*, 1999). Thus, repression of BRCT has implications both in tumourigenic and in defective DNA repair processes. Our results also indicated that DBC1 suppressed BRCA1-dependent transcriptional regulation, because SIRT1-luciferase activity was attenuated by the expression of DBC1. Together with the result of chromatin immunoprecipitation assay, these data suggest the possibility that DBC1 might be involved in the basal transcriptional machinery because BRCA1 associates with RNA polymerase II holoenzyme (Scully *et al*, 1997; Anderson *et al*, 1998). DBC1 would serve as a transcriptional repressive factor to manipulate transcriptions,

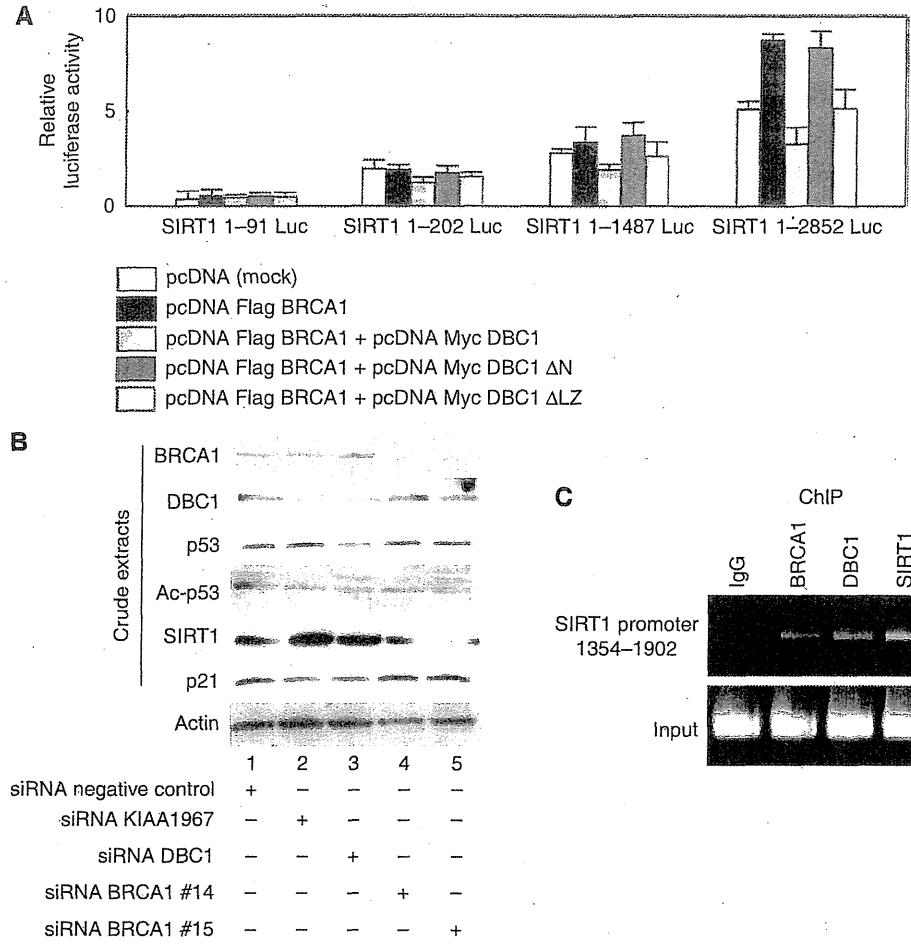

Figure 4 DBC1 represses transcription by BRCA1 through its amino-terminal domain. (**A**) Transient transfection assays were performed to examine the influence of DBC1 using an artificial luciferase reporter construct. Cells (293T) were transfected with the indicated combinations of mammalian expression plasmids. At 24 h after transfection, cells were harvested, and transfected whole-cell lysates were assayed for luciferase activity produced from reporter plasmids. Various lengths of SIRT1 promoter (1–91, 1–202, 1–1487, and 1–2852) were fused upstream of the firefly luciferase reporter plasmid. Full-length DBC1 and DBC1ΔLZ showed specific downregulation of 1–2852 SIRT1-luciferase activity mediated by BRCA1. (**B**) Small interfering RNA (siRNA)-mediated knockdown of BRCA1 decreased the expression of SIRT1. Knockdown of DBC1 resulted in downregulation of acetylated p53 and p21. The expression of SIRT1 was increased by depletion of DBC1. HeLa cells were transfected with indicated siRNA. At 48 h after transfection, cells were harvested and analysed by western blotting. (**C**) Chromatin immunoprecipitation assay was performed to confirm the recruitment of BRCA1 and DBC1 at the SIRT1 gene promoter (1354–1902), a region known to recruit BRCA1 (Wang *et al*, 2008).

thereby influencing transcriptional products such as SIRT1 and p21. Consistent with these results, our recent data have also shown that DBC1 suppresses the ligand-dependent transcriptional activation function of ERβ (Koyama *et al*, 2010).

Apoptosis is a normal physiological process that has an important role in embryonic development and in tissue homoeostasis maintenance. As apoptosis is genetically programmed, its dysfunction contributes to tumour promotion. The previous study showed that BRCA1 is cleaved at amino acid 1151–1154 (DLLD) by caspase-3 during UV-C-induced apoptosis, and the cleaved fragment of BRCA1, containing the BRCT domain, induced cell death through activation of BRCA1 downstream effectors, GADD45 and JNK (Jin *et al*, 2000). Another study reported that DBC1 is translocated from the nucleus to the mitochondria during apoptosis (Sundararajan *et al*, 2005). Thus, our results of immunofluoresence showing that the cleavage of DBC1 and BRCA1 after death signalling promotes their cytoplasmic shuttling indicated that BRCA1 and DBC1 may function synergistically in the apoptotic pathway. It seems reasonable to hypothesise that the cells devoid of nuclear DBC1 staining may be apoptotic. Loss of nuclear DBC1 staining in tissues would be speculated as a marker of therapy efficiency.

The accumulation of DNA damage activates p53 and induces cell-cycle arrest and apoptosis. Acetylation of p53 has been shown to augment p53 DNA binding and to regulate the stability of p53 by inhibiting its ubiquitination by MDM2. In response to DNA damage, acetylation of p53 is stimulated and acetylated p53 enhances its ability to induce cell-cycle arrest, apoptosis, and DNA damage repair (Smith and La Thangue, 2005). Consistent with the previous report by Zhao *et al*, 2008, inactivation of endogenous DBC1 leads to hypoacetylation of p53. This would suggest that abrogation of DBC1 causes malfunctions of p53, including defective DNA repair activities. Furthermore, as we discussed above, repression of the BRCT transactivation function may have significance in impaired DNA damage response. The mechanism by which DBC1 regulates DNA damage machinery seems to be complicated, as DBC1 may possess dual roles in promoting and inhibiting DNA repair, because depletion of DBC1 also results in an increased expression of SIRT1, which possesses DNA repair activity (Jeong *et al*, 2007). We have to further confirm the effect of

DNA damage response when DBC1 is abrogated. Altogether, our results provide new insight into the fact that DBC1 may serve, at least in part, as a DNA damage response machinery.

In conclusion, our data indicate that DBC1 has an important role in regulating BRCA1-mediated functions through binding to the BRCT domain. In addition to its inhibition of the deacetylase activity of SIRT1, DBC1 represses the expression of SIRT1 by associating with BRCA1. DBC1 may be involved both in tumourigenic and anti-tumourigenic processes. This conflicting mechanism can be the reason why expression of DBC1 was not substantially abrogated in various cancers from any type of tissue (Hamaguchi *et al*, 2002). Therefore, both inhibitors and activators of DBC1 would be therapeutically beneficial, by affecting different DBC1-mediated regulatory pathways together with BRCA1. These results suggest that the failure of binding between BRCA1 and DBC1 may be a key event in cancer predisposition.

ACKNOWLEDGEMENTS

This study was supported by a Grant-in-Aid for Scientific Research from the Ministry of Education, Science and Culture, JMS Bayer Schering Pharma Grant, and Kowa Life Science Foundation, Japan. We thank Dr Rui-Hong Wang and Chu-Xia Deng for SIRT1-luciferase vectors, and Dr Ja-Eun Kim for DBC1 ΔLZ construct.

REFERENCES

Anderson SF, Schlegel BP, Nakajima T, Wolpin ES, Parvin JD (1998) BRCA1 protein is linked to the RNA polymerase II holoenzyme complex via RNA helicase A. *Nat Genet* **19:** 254–256

Bork P, Hofmann K, Bucher P, Neuwald AF, Altschul SF, Koonin EV (1997) A superfamily of conserved domains in DNA damage-responsive cell cycle checkpoint proteins. *FASEB J* **11:** 68–76

Callebaut I, Mornon JP (1997) From BRCA1 to RAP1: a widespread BRCT module closely associated with DNA repair. *FEBS Lett* **400:** 25–30

Cha EJ, Noh SJ, Kwon KS, Kim CY, Park BH, Park HS, Lee H, Chung MJ, Kang MJ, Lee DG, Moon WS, Jang KY (2009) Expression of DBC1 and SIRT1 is associated with poor prognosis of gastric carcinoma. *Clin Cancer Res* **15:** 4453–4459

Chapman MS, Verma IM (1996) Transcriptional activation by BRCA1. *Nature* **382:** 678–679

Chen GC, Guan LS, Yu JH, Li GC, Choi Kim HR, Wang ZY (2001) Rb-associated protein 46 (RbAp46) inhibits transcriptional transactivation mediated by BRCA1. *Biochem Biophys Res Commun* **284:** 507–514

Hamaguchi M, Meth JL, von Klitzing C, Wei W, Esposito D, Rodgers L, Walsh T, Welcsh P, King MC, Wigler MH (2002) DBC2, a candidate for a tumor suppressor gene involved in breast cancer. *Proc Natl Acad Sci USA* **99:** 13647–13652

Hohenstein P, Kielman MF, Breukel C, Bennett LM, Wiseman R, Krimpenfort P, Cornelisse C, van Ommen GJ, Devilee P, Fodde R (2001) A targeted mouse Brca1 mutation removing the last BRCT repeat results in apoptosis and embryonic lethality at the headfold stage. *Oncogene* **20:** 2544–2550

Humphrey JS, Salim A, Erdos MR, Collins FS, Brody LC, Klausner RD (1997) Human BRCA1 inhibits growth in yeast: potential use in diagnostic testing. *Proc Natl Acad Sci USA* **94:** 5820–5825

Jeong J, Juhn K, Lee H, Kim SH, Min BH, Lee KM, Cho MH, Park GH, Lee KH (2007) SIRT1 promotes DNA repair activity and deacetylation of Ku70. *Exp Mol Med* **39:** 8–13

Jin S, Zhao H, Fan F, Blanck P, Fan W, Colchagie AB, Fornace Jr AJ, Zhan Q (2000) BRCA1 activation of the GADD45 promoter. *Oncogene* **19:** 4050–4057

Kim JE, Chen J, Lou Z (2008) DBC1 is a negative regulator of SIRT1. *Nature* **451:** 583–586

Koyama S, Wada-Hiraike O, Nakagawa S, Tanikawa M, Hiraike H, Miyamoto Y, Sone K, Oda K, Fukuhara H, Nakagawa K, Kato S, Yano T, Taketani Y (2010) Repression of estrogen receptor β function by putative tumor suppressor DBC1. *Biochem Biophys Res Commun*; e-pub ahead of print 13 January 2010. doi: 10.1016/j.bbrc. 2010. 01. 025

Miyake T, Hu YF, Yu DS, Li R (2000) A functional comparison of BRCA1 C-terminal domains in transcription activation and chromatin remodeling. *J Biol Chem* **275:** 40169–40173

Monteiro AN, August A, Hanafusa H (1996) Evidence for a transcriptional activation function of BRCA1 C-terminal region. *Proc Natl Acad Sci USA* **93:** 13595–13599

Moynahan ME, Chiu JW, Koller BH, Jasin M (1999) Brca1 controls homology-directed DNA repair. *Mol Cell* **4:** 511–518

Oishi H, Kitagawa H, Wada O, Takezawa S, Tora L, Kouzu-Fujita M, Takada I, Yano T, Yanagisawa J, Kato S (2006) An hGCN5/TRRAP histone acetyltransferase complex co-activates BRCA1 transactivation function through histone modification. *J Biol Chem* **281:** 20–26

Ouchi T, Monteiro AN, August A, Aaronson SA, Hanafusa H (1998) BRCA1 regulates p53-dependent gene expression. *Proc Natl Acad Sci USA* **95:** 2302–2306

Saka Y, Esashi F, Matsusaka T, Mochida S, Yanagida M (1997) Damage and replication checkpoint control in fission yeast is ensured by interactions of Crb2, a protein with BRCT motif, with Cut5 and Chk1. *Genes Dev* **11:** 3387–3400

Scully R, Anderson SF, Chao DM, Wei W, Ye L, Young RA, Livingston DM, Parvin JD (1997) BRCA1 is a component of the RNA polymerase II holoenzyme. *Proc Natl Acad Sci USA* **94:** 5605–5610

Smith L, La Thangue NB (2005) Signalling DNA damage by regulating p53 co-factor activity. *Cell Cycle* **4:** 30–32

Somasundaram K, MacLachlan TK, Burns TF, Sgagias M, Cowan KH, Weber BL, el-Deiry WS (1999) BRCA1 signals ARF-dependent stabilization and coactivation of p53. *Oncogene* **18:** 6605–6614

Sundararajan R, Chen G, Mukherjee C, White E (2005) Caspase-dependent processing activates the proapoptotic activity of deleted in breast cancer-1 during tumor necrosis factor-alpha-mediated death signaling. *Oncogene* **24:** 4908–4920

Wada-Hiraike O, Hiraike H, Okinaga H, Imamov O, Barros RP, Morani A, Omoto Y, Warner M, Gustafsson JA (2006) Role of estrogen receptor beta in uterine stroma and epithelium: Insights from estrogen receptor beta−/− mice. *Proc Natl Acad Sci USA* **103:** 18350–18355

Wada O, Oishi H, Takada I, Yanagisawa J, Yano T, Kato S (2004) BRCA1 function mediates a TRAP/DRIP complex through direct interaction with TRAP220. *Oncogene* **23:** 6000–6005

Wang RH, Zheng Y, Kim HS, Xu X, Cao L, Luhasen T, Lee MH, Xiao C, Vassilopoulos A, Chen W, Gardner K, Man YG, Hung MC, Finkel T, Deng CX (2008) Interplay among BRCA1, SIRT1, and survivin during BRCA1-associated tumorigenesis. *Mol Cell* **32:** 11–20

Yarden RI, Brody LC (1999) BRCA1 interacts with components of the histone deacetylase complex. *Proc Natl Acad Sci USA* **96:** 4983–4988

Zhan Q, Jin S, Ng B, Plisket J, Shangary S, Rathi A, Brown KD, Baskaran R (2002) Caspase-3 mediated cleavage of BRCA1 during UV-induced apoptosis. *Oncogene* **21:** 5335–5345

Zhao W, Kruse JP, Tang Y, Jung SY, Qin J, Gu W (2008) Negative regulation of the deacetylase SIRT1 by DBC1. *Nature* **451:** 587–590

Zhong Q, Chen CF, Li S, Chen Y, Wang CC, Xiao J, Chen PL, Sharp ZD, Lee WH (1999) Association of BRCA1 with the hRad50-hMre11-p95 complex and the DNA damage response. *Science* **285:** 747–750

Biochemical and Biophysical Research Communications 392 (2010) 357–362

Contents lists available at ScienceDirect

Biochemical and Biophysical Research Communications

journal homepage: www.elsevier.com/locate/ybbrc

Repression of estrogen receptor β function by putative tumor suppressor DBC1

Satoshi Koyama [a], Osamu Wada-Hiraike [a,*], Shunsuke Nakagawa [a], Michihiro Tanikawa [a], Haruko Hiraike [a], Yuichiro Miyamoto [a], Kenbun Sone [a], Katsutoshi Oda [a], Hiroshi Fukuhara [b], Keiichi Nakagawa [c], Shigeaki Kato [d,e], Tetsu Yano [a], Yuji Taketani [a]

[a] Department of Obstetrics and Gynecology, Graduate School of Medicine, The University of Tokyo, Hongo 7-3-1 Bunkyo-ku, Tokyo 113-8655, Japan
[b] Department of Urology, Graduate School of Medicine, The University of Tokyo, Hongo 7-3-1 Bunkyo-ku, Tokyo 113-8655, Japan
[c] Department of Radiology, Graduate School of Medicine, The University of Tokyo, Hongo 7-3-1 Bunkyo-ku, Tokyo 113-8655, Japan
[d] SORST, Japan Science and Technology, Honcho 4-1-8, Kawaguchi, Saitama 332-0012, Japan
[e] Institute of Molecular and Cellular Biosciences, The University of Tokyo, Yayoi 1-1-1 Bunkyo-ku, Tokyo 113-0034, Japan

ARTICLE INFO

Article history:
Received 5 January 2010
Available online 13 January 2010

Keywords:
DBC1
ERβ
Breast cancer
Transcription
Repression

ABSTRACT

It has been well established that estrogen is involved in the pathophysiology of breast cancer. Estrogen receptor (ER) α appears to promote the proliferation of cancer tissues, while ERβ can protect against the mitogenic effect of estrogen in breast tissue. The expression status of ERα and ERβ may greatly influence on the development, treatment, and prognosis of breast cancer.

Previous studies have indicated that the deleted in breast cancer 1 (DBC1/KIAA1967) gene product has roles in regulating functions of nuclear receptors. The gene encoding DBC1 is a candidate for tumor suppressor identified by genetic search for breast cancer. Caspase-dependent processing of DBC1 promotes apoptosis, and depletion of the endogenous DBC1 negatively regulates p53-dependent apoptosis through its specific inhibition of SIRT1. In addition, DBC1 modulates ERα expression and promotes breast cancer cell survival by binding to ERα.

Here we report an ERβ-specific repressive function of DBC1. Immunoprecipitation and immunofluorescence studies show that ERβ and DBC1 interact in a ligand-independent manner similar to ERα. *In vitro* pull-down assays revealed a direct interaction between DBC1 amino-terminus and activation function-1/2 domain of ERβ. Although DBC1 shows no influence on the ligand-dependent transcriptional activation function of ERα, the expression of DBC1 negatively regulates the ligand-dependent transcriptional activation function of ERβ *in vivo*, and RNA interference-mediated depletion of DBC1 stimulates the transactivation function of ERβ. These results implicate the principal role of DBC1 in regulating ERβ-dependent gene expressions.

Introduction

Estrogen elicits its biological responses via estrogen receptor (ER) α/β-mediated genomic and/or non-genomic pathways. ER is a member of the nuclear receptor (NR) gene superfamily and acts as a ligand-induced transcription factor [1]. ERα and ERβ are stimulated by two distinct activation regions, activation function-1 (AF-1) and AF-2. AF-1, which is located in the amino-terminal A/B domain, is constitutively activated in cell-type and promoter specific manner [2]. AF-2 is located in the carboxyl-terminal ligand binding domain and exerts a ligand-dependent transcriptional activation. AF-1 and AF-2 activate transcription independently and act synergistically [3]. The ligand-dependent activation of ERs requires ligand-dependent association of AF-2 coactivators [4]. An increasing number of molecules which can interact with ERs have been identified and these molecules can modulate biological behavior, e.g. proliferation, growth, sensitivity to apoptotic stimuli, and invasiveness.

Previous studies using knockout mice of ERβ have shown that deficiency of ERβ leads to hyperproliferation and loss of differentiation in epithelia of the uterus [5], ventral prostate [6], and colon [7]. In consistent with *in vivo* studies, *in vitro* studies also suggest the pro-differentiative and anti-proliferative functions of ERβ.

The gene encoding DBC1 was identified during a representative differential analysis to search for candidate breast tumor suppressor genes on a human chromosome 8p21 region frequently deleted in breast cancers [8]. Molecular and cellular function of DBC1 is currently extensively investigated to reveal its physiological role.

Abbreviations: E_2, 17β-estradiol; ER, estrogen receptor; FBS, fetal bovine serum; NLS, nuclear localization signal; NR, nuclear receptor; AF, activation function; GST, glutathione-*S*-transferase

* Corresponding author. Fax: +81 3 3816 2107.
E-mail address: osamuwh-tky@umin.ac.jp (O. Wada-Hiraike).

0006-291X/$ – see front matter © 2010 Elsevier Inc. All rights reserved.
doi:10.1016/j.bbrc.2010.01.025

Endogenous DBC1 is a nuclear protein and is thought to localize in the nucleus depending on its nuclear localization signal (NLS) at the amino-terminus. During TNF-α induced apoptosis, DBC1 is exported to the cytoplasm with loss of the NLS by caspase-dependent cleavage and this processing promotes apoptosis due to the death-promoting activity of its carboxyl-terminal coiled-coil domain [9]. Therefore, caspase-dependent cleavage of DBC1 may act as a positive feedback mechanism to promote apoptosis and possibly also tumor suppression. Recent studies have demonstrated that DBC1 promotes p53-mediated apoptosis through specific inhibition of deacetylase activity of SIRT1, the mammalian homologue of yeast Sir2 (silent information regulator 2) [10,11]. However, the functions of DBC1 in breast cancer still remain largely unknown and it should be determined whether DBC1 plays a pivotal role in tumor suppression.

Current studies have shown that DBC1 interacts with several NRs. DBC1 associates with androgen receptor and facilitates transcriptional activation of androgen receptor [12]. DBC1 stabilizes the interaction between chicken ovalbumin upstream promoter transcription factor I (COUP-TFI) and NCoR by interacting directly with both proteins [13]. DBC1 also interacts with NR complex interacting factor (NRC)-1 to drive the transcription regulation of NRs [14]. On the basis of the report showing that DBC1 is a principal determinant of unliganded ERα expression and promotes proliferation of human breast cancer cells [15], we investigated the functional interaction between DBC1 and ERβ. Our findings reveal that the amino terminus of DBC1 binds directly to ERβ both *in vitro* and *in vivo*. The expression of DBC1 results in a repression of ligand-dependent transcriptional activation function of ERβ. These findings thus may establish a principal biological function for DBC1 in the repression of ERβ function and further underscore DBC1 as a possible endocrine response determinant and potential therapeutic target in breast cancer.

Materials and methods

Cell culture and chemical reagent. ERα positive MCF-7 (HTB-22), ERαβ-positive T47D (HTB-133), and ERβ-positive MDA-MB-231 (HTB-26) human breast cancer cell lines were purchased from the American Type Culture Collection (Manassas, VA, USA). These cells were maintained in Dulbecco's modified Eagle medium (DMEM) supplemented with 10% fetal bovine serum (FBS). DMEM, FBS, and 17β-estradiol (E_2) were purchased from Sigma–Aldrich (St. Louis, MO, USA). ERβ selective ligand, 2,3-bis(4-hydroxyphenyl)-propionitrile (DPN), was from Tocris Bioscience (Ellisville, MO, USA).

Immunoprecipitation. The formation of a DBC1–ERβ complex in MDA-MB-231 cells was analyzed by co-immunoprecipitation using the specific antibodies raised against human ERβ (H-150, Santa Cruz Biotechnology, Santa Cruz, CA, USA), followed by immunoblotting using the anti-human DBC1 (produced in our laboratory). Immunoprecipitation, Western blot analysis, and immunostaining were performed as described previously [16].

Plasmid construction. DBC1 (Clone ID 5496068) and SIRT1 (Clone ID 4518906) expression vectors were purchased from Thermo Fisher Scientific Open Biosystems (Huntsville, AL, USA). Full-length and fragments of DBC1 were inserted into pcDNA-Myc vector derived from pcDNA3 (Invitrogen, Carlsbad, CA, USA). Human ERα AF-1, ERα AF-2, ERβ AF-1, ERβ AF-2 vectors, and a reporter construct (ERE-tk-luc) were described previously [17].

Fluorescence microscopy. MCF-7 and T47D cells were grown on 12 mm BD BioCoat glass coverslips in 6-well plates. These cells

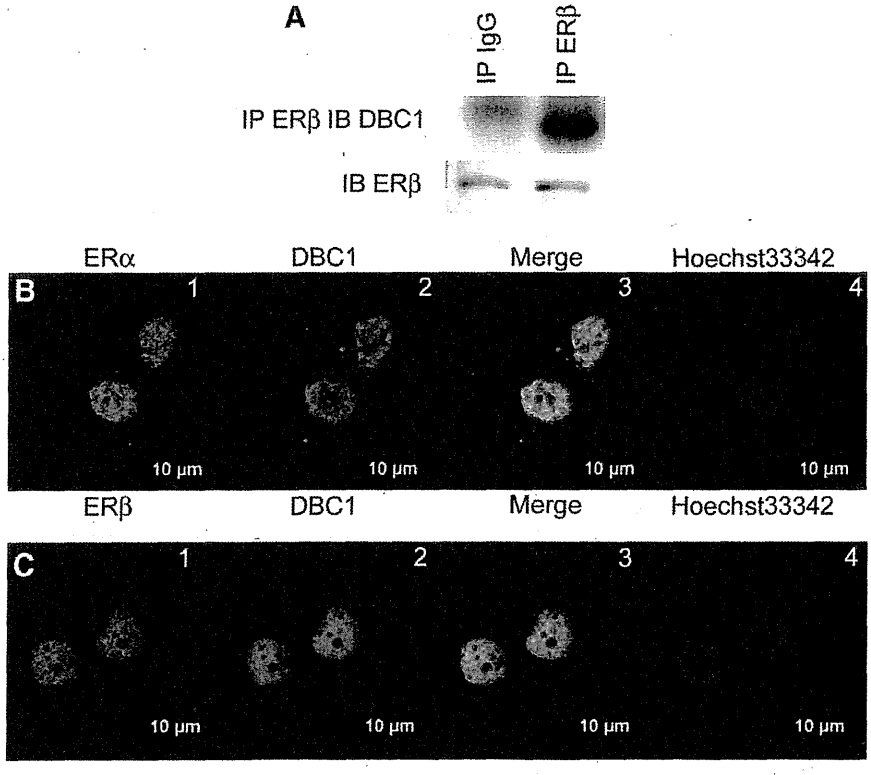

Fig. 1. *In vivo* association between DBC1 and ERα/β. (A) The formation of a DBC1 and ERβ complex in MDA-MB-231 cells was analyzed by co-immunoprecipitation (IP) with the antbodies to ERβ or preimmune IgG, followed by immunoblotting (IB) using the anti-DBC1 antibody. The immunoprecipitates were subjected to 30 μl of protein G sepharose™ 4 Fast Flow and detected by Western blotting. (B) MCF-7 cells were fixed and permeabilized. The cells were incubated with primary antibodies and subsequently with secondary antibodies. B1, ERα; B2, DBC1; B3, merge; B4, Hoechst 33342 staining. (C) T47D cells were incubated with primary antibodies and secondary antibodies. C1, ERβ; C2, DBC1; C3, merge; C4, Hoechst 33342 staining. Expression of DBC1 (red) and ERs (green) were investigated under the confocal fluorescence microscopy. Bars indicate 10 μm.

were maintained in DMEM supplemented with 10% FBS. Cells were fixed with PBS containing 4% paraformaldehyde and permeabilized in PBS with 0.2% (v/v) Triton X-100. After blocking, MCF-7 cells were incubated with anti-ERα (D-12, Santa Cruz Biotechnology) and anti-DBC1 antibodies. T47D cells were incubated with anti-ERβ (14C8, Novus Biologicals Inc., Littleton, CO, USA) and anti-DBC1 antibodies. Secondary antibodies were Alexa fluor 488 conjugated donkey anti-mouse IgG, and Alexa fluor 555 conjugated goat anti-rabbit IgG. The slides were briefly counter-stained and analyzed under the confocal fluorescence microscope (Carl-Zeiss MicroImaging Inc., Oberkochen, Germany).

GST-pull down assay. GST fusion proteins or GST alone were expressed in *Escherichia coli* and bound to glutathione-sepharose 4B beads (GE healthcare UK Ltd., Buckinghamshire, UK). Immobilized GST-ERα/β AF-2 fusion proteins were preincubated for 30 min in GST binding buffer (20 mM Tris–HCl pH 7.5, 200 mM NaCl, 1 mM EDTA) with E_2 (10^{-6} M). The GST proteins were incubated at 4 °C with indicated [^{35}S] methionine-labeled proteins. After 1 h incubation, unbound proteins were removed by washing the beads in GST binding buffer containing 0.5% Nonidet P-40 and proteases inhibitor cocktail. Specifically bound proteins were eluted by boiling in SDS sample buffer and analyzed by 7~12% SDS–polyacrylamide gel electrophoresis and autoradiography.

Luciferase assay. Two days before transfection, the medium was changed to phenol red-free DMEM containing 5% charcoal stripped FBS. Transfection was performed with Effectene reagent (Qiagen, Hilden, Germany) according to the manufacturer's recommendation. For luciferase assay, 250 ng ERE-tk-luc plasmid was cotransfected with indicated expression vectors. As an internal control to equalize transfection efficiency, 1 ng of phRL CMV luc vector (Promega Co., Madison, WI, USA) was cotransfected in all the experiments. Individual transfections, each consisting of triplicate wells, were repeated at least three times [16].

RNAi. The ablation of DBC1 was performed by the transfection of MDA-MB-231 cells with either of two siRNA duplex oligos synthesized by Qiagen. Either of two DBC1-specific siRNA (DBC1-RNAi: 5′ AAACGGAGCCUACUGAACA 3′, which covered mRNA regions of nucleotides 1379–1397 (amino acids 460–466) of DBC1 or KIAA1967-RNAi: 5′-CGCUUAUAGUUCGAAGGUA-3′, SI00461853), or control siRNA (All Stars Negative Control siRNA, 1027281) was transfected by using HyperFect reagent (Qiagen).

RNA extraction and real-time quantitative PCR. MDA-MB-231 cells were transfected with pcDNA3 (control) or pcDNA Myc DBC1. The cells were treated with vehicle (Ethanol), E_2 (10^{-9} M), or DPN (10^{-8} M) and incubated for subsequent 24 h. Total RNA was extracted from the cells using RNeasy Mini Kit (Qiagen) and real-time quantitative PCR was performed. The amplification of Bcl-2 mRNA was performed using primers for cDNA of Bcl-2, upstream 5′-AGGATTGTGGCCTTCTTTGAG-3′ and downstream 5′-CCTGCAGCTTTGTTTCATGGT-3′ [18]. Bcl-2 mRNA levels were normalized to RNA loading for each sample using glyceraldehyde-3-phosphate dehydrogenase (GAPDH) mRNA as an internal standard. Data analyses were performed using a Light Cycler (Roche Applied Science, Mannheim, Germany).

Results

ERβ and DBC1 interact in vivo

The fact that endogenous ERα and DBC1 interacts in the absence of E_2 led us to examine whether DBC1 protein interacts with ERβ in cultured human cells. ERβ was immunoprecipitated in MDA-MB-231 cell lysates and a complex formation of the precipitated proteins was confirmed by Western blotting. Immunoblotting revealed the existence of DBC1 in the cell lysate immunoprecipitates (Fig. 1A), which supports our hypothesis that DBC1 physically associates with ERβ in living cells. This result was further confirmed by immunofluorescence studies using the specific antibodies raised against ERβ and DBC1. Immunofluorescence staining revealed the ligand-independent colocalization of ERβ and DBC1 in the nucleus of T47D cells (Fig. 1C, 1–4). As expected from the previous study, ERα and DBC1 showed ligand-independent colocalization in the nucleus of MCF-7 cells (Fig. 1B, 1–4).

ERαβ and DBC1 interact in vitro in a ligand-independent manner

To address the functional importance of the DBC1–ERβ interaction, *in vitro* translated [^{35}S] methionine labeled DBC1 was incu-

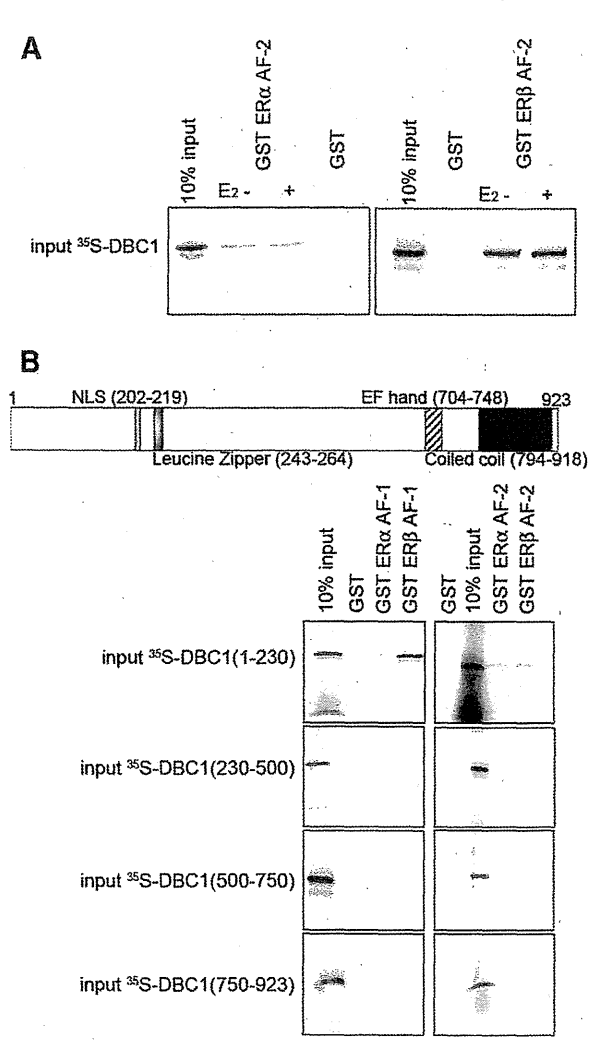

Fig. 2. *In vitro* association between DBC1 and ERαβ, and mapping of the ERβ-interacting region of DBC1. (A) Ligand independent association between full-length DBC1 and AF-2 region of ERαβ using GST-ERαβ AF-2 and DBC1. Bacterially expressed GST fusion proteins immobilized on beads were used in *in vitro* pull-down assays. Full-length DBC1 was *in vitro* translated in the presence of [^{35}S] methionine using a TNT coupled *in vitro* translation system. Labeled DBC1 was then incubated with GST-ERαβ AF-2. GST-ERαβ AF-2 was treated with or without 10^{-6} M of E_2. The mixture was washed and subjected to SDS–PAGE and analyzed. (B) Mapping of the DBC1-interaction region of ERαβ using GST-ERαβ AF-1, GST-ERαβ AF-2, and fragments of DBC1. DBC1 amino acids 1–230, 230–500, 500–750, and 750–923 were *in vitro* translated. The fragments of DBC1 and GST-ERαβ AF-1 and AF-2 were tested for interaction. The mixture was washed and subjected to SDS–PAGE and then visualized by autoradiography. Polyacrylamide gels were stained briefly with Coomassie Brilliant Blue to verify the loading of equal amounts of fusion proteins prior to drying and autoradiography.

bated with GST-fused ERαβ AF-2. As clearly shown in Fig. 2A, GST-fused ERαβ AF-2 protein possessed the ability to retain DBC1 on the column in the presence and absence of E_2.

To map the region of DBC1 that interacts with ERαβ, GST-fused ERαβ AF-1 or AF-2 and *in vitro* translated DBC1 fragments, (1–230 amino acids), (230–500), (500–750), and (750–923), were incubated and tested for the interaction. Only amino-terminus of DBC1 including the NLS interacted with ERαβ AF-2 in a ligand-independent manner. Interestingly, ERαβ AF-1 showed different interaction pattern because the GST ERβ AF-1 column exhibited significantly stronger interaction with amino-terminus of DBC1 compared with GST ERα AF-1 column (Fig. 2B).

DBC1 exhibits no influence on the transcriptional activation function of ERα

To examine the cofactor activity of DBC1 in the transactivation function of ERα, transient transfection assays were performed using a luciferase reporter plasmid driven by the thymidine kinase promoter containing estrogen responsive element (ERE-tk-luc). Although ERα showed a ligand-dependent transactivation function in 293T cells, a transient coexpression of DBC1 showed no influence on the luciferase activity of ERα (Fig. 3A). Role of SIRT1 in regulating transactivation of ERα was confirmed and the expression of SIRT1 decreased luciferase activity of ERα (Fig. 3A). The transcriptional regulation of ERα played by DBC1 was further confirmed in MDA-MB-231 cells (Fig. 3B). The ligand-induced transactivation function of ERα was unaffected by short-interference RNA (siRNA) mediated depletion of DBC1 (Fig. 3B).

DBC1 represses the transcriptional activation function of ERβ

The cofactor activity of DBC1 in the transactivation function of ERβ was further confirmed. Although ERβ showed a ligand-dependent transactivation function in 293T cells, a transient coexpression of DBC1 led to a significant decrease in luciferase activity of ERβ (Fig. 4A and B). Role of SIRT1 in regulating transactivation of ERβ was analyzed but the luciferase activity of ERβ was unaffected by the expression of SIRT1 unlike ERα. This downregulation of transactivation by DBC1 was further confirmed in MDA-MB-231 cells. The ligand-induced transactivation function of ERβ was stimulated by transfecting siRNA of DBC1 (Fig. 4B). To evaluate the effect of DBC1 on the endogenous gene expression, mRNA expression of Bcl-2 was examined because this anti-apoptotic gene has been shown to be an ERβ-repressed gene in the ventral prostate [6]. The transient expression of DBC1 resulted in an increase of Bcl-2 mRNA in the presence of ERβ ligands, namely, E_2 or DPN (Fig. 4C). These data indicate a significant role of DBC1 in the ligand-dependent repression function of ERβ.

Discussion

The recent study has shown that the overexpression of DBC1 and SIRT1 are related to the poorer prognosis in gastric cancer patients [19]. In addition, the expression of DBC1 was not substantially abrogated in various cancers from any tissue [15]. Even though DBC1 was originally identified as a candidate for breast tumor suppressor gene, it remains unknown whether the aberrant expression of DBC1 is correlated with carcinogenesis. The precise molecular and cellular mechanisms of DBC1 in tumorigenesis should be solved to understand the physiological function of DBC1. Not only the interaction between ERα and DBC1 [15], but the interaction between ERβ and DBC1 may have a significant role in the pathogenesis of breast cancer. ERβ plays a multifaceted role in the functional differentiation of various epithelial and non-epithelial cell types and ERβ seems to be essential for driving cellular differentiation and apoptosis. Many studies to find correlations between breast tumorigenesis and ERs have been conducted, and an increase in ERα/ERβ ratio in breast cancer as compared with benign tumors and normal tissues has been reported [20–22]. These studies indicate that healthy mammary glands express more ERβ mRNA than do breast cancer samples. A number of *in vitro* functional studies have been performed to examine the effect of ERβ expression on the proliferation of breast cancer cells [23,24]. Although the results are not unanimous, the majority of studies conclude that an increase in ERβ expression decreases cell proliferation. All these observations suggest that loss of the expression of ERβ may be involved in tumor progression. The American Association for Cancer Research Task Force Report has mentioned ERβ as a possible target for chemoprevention in a number of cancers, including breast cancer [25]. Several ERβ selective ligands such as DPN [26], ERB-41 [27], and TAS-108 [28] have been developed and evaluated *in vivo*. Among them, TAS-108 is a selective ERα antagonist with partial ERβ agonist activity, and a Phase I clinical trial using

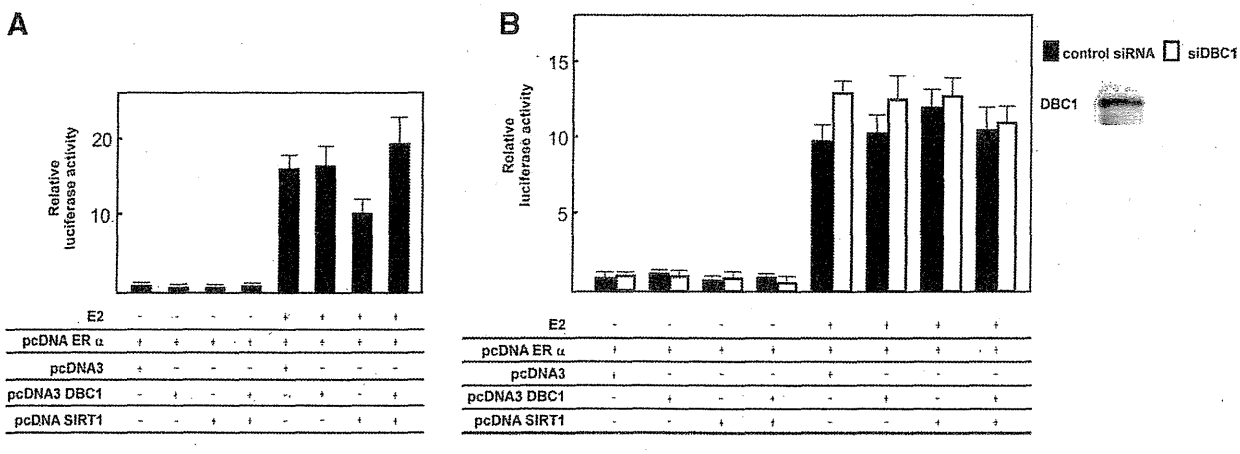

Fig. 3. DBC1 shows no influence on ligand-dependent transcriptional activation function of ERα. (A) Transient transfection assays were performed to examine the activity of DBC1 in the transactivation function of ERα. The expression of DBC1 showed no effect on the ligand-dependent transactivation function of ERα in 293T cells. (B) siRNA-mediated depletion of the endogenous DBC1 was performed in MDA-MB-231 cells. The cells were transfected with siRNA specific for DBC1. Forty-eight hours after transfection, the cells were transfected with indicated expression vectors and reporter constructs. Twenty-four hours after transfection of expression vectors and reporter constructs (ERE-tk-luc), cells were harvested, and transfected whole cell lysates were assayed for luciferase activity produced from the reporter plasmid.

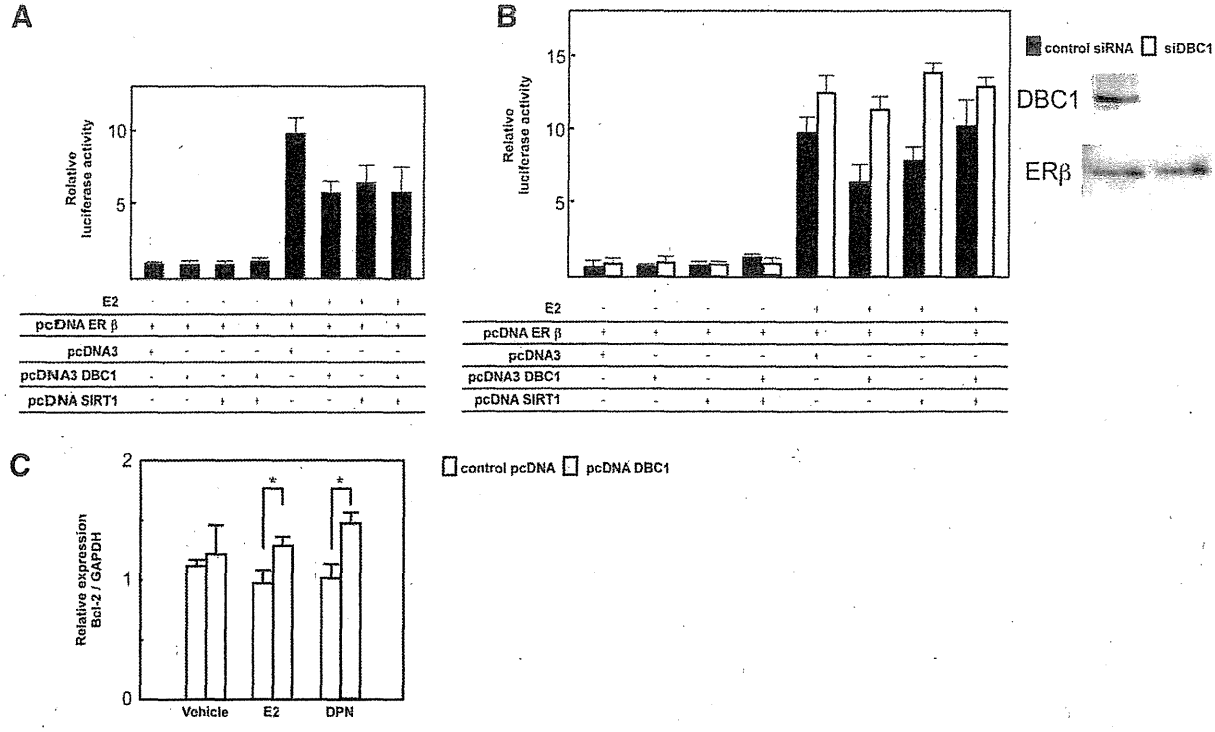

Fig. 4. DBC1 attenuates ligand-dependent transcription activation function of ERβ. (A) Transient transfection assays were performed to examine the activity of DBC1 in the transactivation function of ERβ. DBC1 showed a specific repression of ligand-dependent transactivation function of ERβ in 293T cells. (B) The repression function of DBC1 was reversed by siRNA-mediated depletion of the endogenous DBC1. MDA-MB-231 cells were transfected with siRNA specific for DBC1. Forty-eight hours after transfection, the cells were transfected with indicated expression vectors and reporter constructs. The expression of ERβ was unaffected by the siRNA-mediated knockdown of DBC1. (C) In the presence of E_2 and DPN, the expression of Bcl-2 mRNA was stimulated by transfecting the expression vector of DBC1.

TAS-108 has been conducted with promising results [29]. Therefore, the expression of ERβ and the stimulation of ERβ transcriptional activity have significant roles in the pathophysiology of tumor development. Our findings have demonstrated a novel role of DBC1 in repressing the transcriptional function of ERβ. This ligand-dependent repression function of DBC1 was confirmed by the expression of Bcl-2, an ERβ-repressed gene, and Bcl-2 was increased in a ligand-dependent manner. In contrast to the previous report [15], ERα AF-2 exhibited physical association with DBC1 irrespective of the presence of E_2. Although ERβ AF-2 also associated with DBC1 in a ligand-independent manner, DBC1 exhibited completely different transcriptional regulation of ERβ compared to that of ERα. This difference may be attributed to the fact that ERβ AF-1 showed robust interaction with DBC1. Taking into account of these data, DBC1 might be an ERβ-specific transcriptional repressor. We speculate that the DBC1–ERα complex formation would be related to hormone-independent tumor growth and the DBC1–ERβ complex formation would be related to hormone-dependent tumor growth. These complex formations between ERαβ and DBC1 would be tumorigenic and this fact would have implications for breast cancer prognosis and/or treatment. It is believed that a balance between proliferation (ERα) and apoptosis (ERβ) influences the response of breast tumors to hormonal therapy, and dysregulation of apoptotic signaling pathways has been suggested as a possible basis for treatment failure. Alterations in the expression and activity of ERs by DBC1 could tip the balance between breast tumor formation and death signaling. Further investigations are needed to elucidate the molecular mechanisms that underlie the formation of ERαβ–DBC1 in normal cellular growth, thereby evaluating DBC1 as a possible target for modality of prevention and medical treatment of breast cancer.

Acknowledgments

This study was supported by Grant-in-Aid for Scientific Research from the Ministry of Education, Science and Culture, JMS Bayer Schering Pharma Grant, and Kowa Life Science Foundation, Japan.

References

[1] D.J. Mangelsdorf, C. Thummel, M. Beato, P. Herrlich, G. Schutz, K. Umesono, B. Blumberg, P. Kastner, M. Mark, P. Chambon, R.M. Evans, The nuclear receptor superfamily: the second decade, Cell 83 (1995) 835–839.
[2] D. Metzger, S. Ali, J.M. Bornert, P. Chambon, Characterization of the amino-terminal transcriptional activation function of the human estrogen receptor in animal and yeast cells, J. Biol. Chem. 270 (1995) 9535–9542.
[3] G.N. Lopez, P. Webb, J.H. Shinsako, J.D. Baxter, G.L. Greene, P.J. Kushner, Titration by estrogen receptor activation function-2 of targets that are downstream from coactivators, Mol. Endocrinol. 13 (1999) 897–909.
[4] D.M. Lonard, B.W. O'Malley, The expanding cosmos of nuclear receptor coactivators, Cell 125 (2006) 411–414.
[5] O. Wada-Hiraike, H. Hiraike, H. Okinaga, O. Imamov, R.P. Barros, A. Morani, Y. Omoto, M. Warner, J.A. Gustafsson, Role of estrogen receptor beta in uterine stroma and epithelium: insights from estrogen receptor beta−/− mice, Proc. Natl. Acad. Sci. USA 103 (2006) 18350–18355.
[6] O. Imamov, A. Morani, G.J. Shim, Y. Omoto, C. Thulin-Andersson, M. Warner, J.A. Gustafsson, Estrogen receptor beta regulates epithelial cellular differentiation in the mouse ventral prostate, Proc. Natl. Acad. Sci. USA 101 (2004) 9375–9380.
[7] O. Wada-Hiraike, O. Imamov, H. Hiraike, K. Hultenby, T. Schwend, Y. Omoto, M. Warner, J.A. Gustafsson, Role of estrogen receptor beta in colonic epithelium, Proc. Natl. Acad. Sci. USA 103 (2006) 2959–2964.
[8] M. Hamaguchi, J.L. Meth, C. von Klitzing, W. Wei, D. Esposito, L. Rodgers, T. Walsh, P. Welcsh, M.C. King, M.H. Wigler, DBC2, a candidate for a tumor suppressor gene involved in breast cancer, Proc. Natl. Acad. Sci. USA 99 (2002) 13647–13652.
[9] R. Sundararajan, G. Chen, C. Mukherjee, E. White, Caspase-dependent processing activates the proapoptotic activity of deleted in breast cancer-1 during tumor

necrosis factor-alpha-mediated death signaling, Oncogene 24 (2005) 4908–4920.
[10] J.E. Kim, J. Chen, Z. Lou, DBC1 is a negative regulator of SIRT1, Nature 451 (2008) 583–586.
[11] W. Zhao, J.P. Kruse, Y. Tang, S.Y. Jung, J. Qin, W. Gu, Negative regulation of the deacetylase SIRT1 by DBC1, Nature 451 (2008) 587–590.
[12] J. Fu, J. Jiang, J. Li, S. Wang, G. Shi, Q. Feng, E. White, J. Qin, J. Wong, Deleted in breast cancer 1, a novel androgen receptor (AR) coactivator that promotes AR DNA-binding activity, J. Biol. Chem. 284 (2009) 6832–6840.
[13] L.J. Zhang, X. Liu, P.R. Gafken, C. Kioussi, M. Leid, A chicken ovalbumin upstream promoter transcription factor I (COUP-TFI) complex represses expression of the gene encoding tumor necrosis factor alpha-induced protein 8 (TNFAIP8), J. Biol. Chem. 284 (2009) 6156–6168.
[14] S. Garapaty, C.F. Xu, P. Trojer, M.A. Mahajan, T.A. Neubert, H.H. Samuels, Identification and characterization of a novel nuclear protein complex involved in nuclear hormone receptor-mediated gene regulation, J. Biol. Chem. 284 (2009) 7542–7552.
[15] A.M. Trauernicht, S.J. Kim, N.H. Kim, T.G. Boyer, Modulation of estrogen receptor alpha protein level and survival function by DBC-1, Mol. Endocrinol. 21 (2007) 1526–1536.
[16] O. Wada-Hiraike, T. Yano, T. Nei, Y. Matsumoto, K. Nagasaka, S. Takizawa, H. Oishi, T. Arimoto, S. Nakagawa, T. Yasugi, S. Kato, Y. Taketani, The DNA mismatch repair gene hMSH2 is a potent coactivator of oestrogen receptor alpha, Br. J. Cancer 92 (2005) 2286–2291.
[17] T. Fujita, Y. Kobayashi, O. Wada, Y. Tateishi, L. Kitada, Y. Yamamoto, H. Takashima, A. Murayama, T. Yano, T. Baba, S. Kato, Y. Kawabe, J. Yanagisawa, Full activation of estrogen receptor alpha activation function-1 induces proliferation of breast cancer cells, J. Biol. Chem. 278 (2003) 26704–26714.
[18] A. Castro, M.C. Johnson, M. Anido, A. Cortinez, F. Gabler, M. Vega, Role of nitric oxide and bcl-2 family genes in the regulation of human endometrial apoptosis, Fertil Steril 78 (2002) 587–595.
[19] E.J. Cha, S.J. Noh, K.S. Kwon, C.Y. Kim, B.H. Park, H.S. Park, H. Lee, M.J. Chung, M.J. Kang, D.G. Lee, W.S. Moon, K.Y. Jang, Expression of DBC1 and SIRT1 is associated with poor prognosis of gastric carcinoma, Clin. Cancer Res. 15 (2009) 4453–4459.
[20] P. Roger, M.E. Sahla, S. Makela, J.A. Gustafsson, P. Baldet, H. Rochefort, Decreased expression of estrogen receptor beta protein in proliferative preinvasive mammary tumors, Cancer Res. 61 (2001) 2537–2541.
[21] J.A. Shaw, K. Udokang, J.M. Mosquera, H. Chauhan, J.L. Jones, R.A. Walker, Oestrogen receptors alpha and beta differ in normal human breast and breast carcinomas, J. Pathol. 198 (2002) 450–457.
[22] B.W. Park, K.S. Kim, M.K. Heo, S.S. Ko, S.W. Hong, W.I. Yang, J.H. Kim, G.E. Kim, K.S. Lee, Expression of estrogen receptor-beta in normal mammary and tumor tissues: is it protective in breast carcinogenesis?, Breast Cancer Res Treat. 80 (2003) 79–85.
[23] Y. Omoto, H. Eguchi, Y. Yamamoto-Yamaguchi, S. Hayashi, Estrogen receptor (ER) beta1 and ERbetacx/beta2 inhibit ERalpha function differently in breast cancer cell line MCF7, Oncogene 22 (2003) 5011–5020.
[24] D.A. Tonetti, R. Rubenstein, M. DeLeon, H. Zhao, S.G. Pappas, D.J. Bentrem, B. Chen, A. Constantinou, V. Craig Jordan, Stable transfection of an estrogen receptor beta cDNA isoform into MDA-MB-231 breast cancer cells, J. Steroid Biochem. Mol. Biol. 87 (2003) 47–55.
[25] G.J. Kelloff, S.M. Lippman, A.J. Dannenberg, C.C. Sigman, H.L. Pearce, B.J. Reid, E. Szabo, V.C. Jordan, M.R. Spitz, G.B. Mills, V.A. Papadimitrakopoulou, R. Lotan, B.B. Aggarwal, R.S. Bresalier, J. Kim, B. Arun, K.H. Lu, M.E. Thomas, H.E. Rhodes, M.A. Brewer, M. Follen, D.M. Shin, H.L. Parnes, J.M. Siegfried, A.A. Evans, W.J. Blot, W.H. Chow, P.L. Blount, C.C. Maley, K.K. Wang, S. Lam, J.J. Lee, S.M. Dubinett, P.F. Engstrom, F.L. Meyskens Jr., J. O'Shaughnessy, E.T. Hawk, B. Levin, W.G. Nelson, W.K. Hong, Progress in chemoprevention drug development: the promise of molecular biomarkers for prevention of intraepithelial neoplasia and cancer—a plan to move forward, Clin. Cancer Res. 12 (2006) 3661–3697.
[26] M.J. Meyers, J. Sun, K.E. Carlson, G.A. Marriner, B.S. Katzenellenbogen, J.A. Katzenellenbogen, Estrogen receptor-beta potency-selective ligands: structure–activity relationship studies of diarylpropionitriles and their acetylene and polar analogues, J. Med. Chem. 44 (2001) 4230–4251.
[27] M.S. Malamas, E.S. Manas, R.E. McDevitt, I. Gunawan, Z.B. Xu, M.D. Collini, C.P. Miller, T. Dinh, R.A. Henderson, J.C. Keith Jr., H.A. Harris, Design and synthesis of aryl diphenolic azoles as potent and selective estrogen receptor-beta ligands, J. Med. Chem. 47 (2004) 5021–5040.
[28] Y. Yamamoto, J. Shibata, K. Yonekura, K. Sato, A. Hashimoto, Y. Aoyagi, K. Wierzba, S. Yano, T. Asao, A.U. Buzdar, T. Terada, TAS-108, a novel oral steroidal antiestrogenic agent, is a pure antagonist on estrogen receptor alpha and a partial agonist on estrogen receptor beta with low uterotrophic effect, Clin. Cancer Res. 11 (2005) 315–322.
[29] L.J. Blakely, A. Buzdar, H.Y. Chang, D. Frye, R. Theriault, V. Valero, E. Rivera, D. Booser, J. Kuritani, M. Tsuda, A phase I and pharmacokinetic study of TAS-108 in postmenopausal female patients with locally advanced, locally recurrent inoperable, or progressive metastatic breast cancer, Clin. Cancer Res. 10 (2004) 5425–5431.

Oncogene (2010) 29, 1897–1908

www.nature.com/onc

ORIGINAL ARTICLE

Genome-wide single-nucleotide polymorphism arrays in endometrial carcinomas associate extensive chromosomal instability with poor prognosis and unveil frequent chromosomal imbalances involved in the PI3-kinase pathway

S Murayama-Hosokawa[1,2,5], K Oda[2,5], S Nakagawa[2], S Ishikawa[1,3], S Yamamoto[1], K Shoji[2], Y Ikeda[2], Y Uehara[1,2], M Fukayama[3], F McCormick[4], T Yano[2], Y Taketani[2] and H Aburatani[1]

[1]Genome Science Division, Research Center for Advanced Science and Technology, The University of Tokyo, Tokyo, Japan; [2]Department of Obstetrics and Gynecology, The University of Tokyo, Tokyo, Japan; [3]Department of Pathology, The University of Tokyo, Tokyo, Japan and [4]UCSF Helen Diller Family Comprehensive Cancer Center and Cancer Research Institute, University of California, San Francisco, CA, USA

Endometrial cancer is one of the tumor types in which either chromosomal instability (CIN) or microsatellite instability (MSI) may occur. It is known to possess mutations frequently in the Ras-PI3K (phosphatidylinositol 3′-kinase) pathway. We performed a comprehensive genomic survey in 31 endometrial carcinomas with paired DNA for chromosomal imbalances (25 by the 50K and 6 by the 250K single-nucleotide polymorphism (SNP) array), and screened 25 of the 31 samples for MSI status and mutational status in the Ras-PI3K pathway genes. We detected five or more copy number changes (classified as CIN-extensive) in 9 (29%), 1 to 4 changes (CIN-intermediate) in 17 (55%) and no changes (CIN-negative) in 5 (16%) tumors. Positive MSI was less common in CIN-extensive tumors (14%), compared with CIN-intermediate/negative tumors (50%), and multivariate analysis showed that CIN-extensive is an independent poor prognostic factor. SNP array analysis unveiled copy number neutral LOH at 54 loci in 13 tumors (42%), including four at the locus of *PTEN*. In addition to eight (26%) tumors with *PTEN* deletions, we detected chromosomal imbalances of *NF1*, *K-Ras* and *PIK3CA* in four (13%), four (13%) and six (19%) tumors, respectively. In all, 7 of the 9 CIN-extensive tumors harbor deletions in the loci of *PTEN* and/or *NF1*, whereas all the 10 MSI-positive tumors possess *PTEN*, *PIK3CA* and/or *K-Ras* mutations. Our results showed that genomic alterations in the Ras-PI3K pathway are remarkably widespread in endometrial carcinomas, regardless of the type of genomic instability, and suggest that the degree of CIN is a useful biomarker for prognosis in endometrial carcinomas.

Oncogene (2010) **29**, 1897–1908; doi:10.1038/onc.2009.474; published online 11 January 2010

Keywords: chromosomal instability; microsatellite instability; copy number neutral LOH; homozygous deletions; Ras-PI3K pathway; endometrial carcinoma

Correspondence: Professor H Aburatani, Genome Science Division, Research Center for Advanced Science and Technology, The University of Tokyo, Komaba 4-6-1, Meguro, Tokyo 153-8904, Japan. E-mail: haburata-tky@umin.ac.jp
[5]These authors contributed equally to this work.
Received 27 June 2009; revised 7 November 2009; accepted 19 November 2009; published online 11 January 2010

Introduction

Genomic alterations, such as DNA sequence changes, genomic instability and epigenetic gene silencing, cooperate to develop and progress human malignancies. Understanding the molecular basis of cancer has now become feasible through the application of genome analysis technologies, as in a project started by The Cancer Genome Atlas (Cancer Genome Atlas Research Network, 2008).

Endometrial cancer is the fourth most frequent cancer in women and its incidence is increasing (Parkin, 2001). There are two different pathogenetic types of endometrial carcinomas: estrogen-dependent type I and estrogen-independent type II (Ryan *et al.*, 2005; Doll *et al.*, 2008). Approximately, 80% of endometrial carcinomas are endometrioid adenocarcinomas, generally considered as type I tumors. Type II is composed of high-grade tumors (such as serous adenocarcinomas or clear cell carcinomas) with aggressive behavior. Even among type I tumors, recurrent tumors respond limitedly to systemic therapy and the prognosis is very poor. Microsatellite instability (MSI) is associated with mutator phenotype, and is reported approximately at 15–20% in endometrial and colorectal cancer (Atkin, 2001; Woerner *et al.*, 2003). MSI in endometrial cancer is much more frequent in type I endometrioid adenocarcinomas than in type II tumors (Tashiro *et al.*, 1997; An *et al.*, 2004). Chromosomal instability (CIN) is measured by the number of chromosomal copy alterations within entire tumor genomes, and the CIN phenotypes can be classified according to the level of alterations, such as CIN-high, CIN-low and CIN-very low (Rowan *et al.*, 2005; Weber *et al.*, 2007; Geigl *et al.*, 2008). CIN is inversely correlated with MSI in colorectal cancer (Choi

et al., 2002; Grady, 2004); however, the relationship between CIN and MSI and its prognostic effect in type I endometrioid adenocarcinomas is still controversial (Hirasawa *et al.*, 2003; Arabi *et al.*, 2009). We especially focused on endometrioid adenocarcinomas to clarify whether the status of genomic instability, determined by CIN and MSI analyses, is associated with morphologically indistinguishable tumor aggressiveness.

Copy number neutral (CNN) LOH is a type of genomic alteration caused by the loss of one allele and gain of the opposite allele. Recently, single-nucleotide polymorphism (SNP) arrays, which could provide allele-specific copy number information, have been applied to detect segmental uniparental structures (Fitzgibbon *et al.*, 2005; Teh *et al.*, 2005; Midorikawa *et al.*, 2006). Somatic CNN LOH has been increasingly recognized as a common molecular defect in various types of cancer. In addition, improvement of resolution by SNP arrays is also useful in identifying microdeletions, including homozygous deletions (HDs) (Komura *et al.*, 2006; Gorringe *et al.*, 2007). SNP array analyses have unveiled that regions surrounding various tumor suppressor genes (such as *CDKN2A*, *RB1*, *TP53*, *BRCA1*, *BRCA2*, *WT1*, *CEBPA*, *RUNX1* and *NF1*) frequently show CNN LOH in many types of tumors (Fitzgibbon *et al.*, 2005; Raghavan *et al.*, 2005; Flotho *et al.*, 2007; Walsh *et al.*, 2008). Recent studies also indicate that CNN LOH regions may carry activated oncogenes, such as mutated *JAK2*, *HRAS* and *NRAS* (Kralovics *et al.*, 2005; Kratz *et al.*, 2007; Dunbar *et al.*, 2008). Thus, SNP array is a useful methodology to identify novel genomic alterations in specific genes and pathways.

The phosphatidylinositol 3′-kinases (PI3Ks) are widely expressed lipid kinases that catalyze the production of the second messenger phosphatidylinositol 3,4, 5-triphosphate, which activates a wide range of downstream targets, including Akt (Stokoe *et al.*, 1997). Ras-PI3K signaling is activated through various genetic alterations, such as mutations in *Ras*, *PTEN*, *EGFR*, *PIK3CA* and *AKT1* (Vogelstein *et al.*, 1988; Li *et al.*, 1997; Lynch *et al.*, 2004; Samuels *et al.*, 2004; Carpten *et al.*, 2007), and amplifications in *ERBB2*, *AKT2* and *PIK3CA* (Slamon *et al.*, 1989; Cheng *et al.*, 1992; Shayesteh *et al.*, 1999). In endometrial cancer, high prevalence of mutations of the genes in the Ras-PI3K pathway is reported, including *K-Ras*, *PTEN* and *PIK3CA* (Enomoto *et al.*, 1991; Kong *et al.*, 1997; Oda *et al.*, 2005). We reported that more than 70% of endometrial carcinomas contain one or more mutations in the Ras-PI3K pathway (Oda *et al.*, 2008). However, the role of chromosomal imbalances in this pathway is not fully understood. Various kinds of inhibitors targeting the PI3K pathway have been developed and are now under clinical trials (Kong and Yamori, 2008; Maira *et al.*, 2009). Detailed analysis of genomic alterations in this pathway might clarify the possibility of these molecular targeted therapies in endometrial carcinomas.

In this study, we attempted to comprehensively figure out genomic alterations in endometrial carcinomas. First, we classified endometrial carcinomas into three subgroups according to the CIN status, and found an inverse trend between the high degree of CIN (CIN-extensive) and positive MSI. Second, we show that CIN-extensive is an independent poor prognostic predictor in endometrial carcinomas. Third, we focused on the genes involved in the Ras-PI3K pathway for mutations, CNN LOH, HD and other chromosomal imbalances and clarified that genomic alterations associated with the Ras-PI3K pathway are exceedingly widespread in endometrial carcinomas.

Results

Chromosomal gains, losses, CNN LOH and HDs in endometrial carcinomas

As endometrioid adenocarcinoma is the most common histological type showing a high ratio of MSI, we specifically focused on endometrioid adenocarcinomas in this study. We evaluated chromosomal imbalances in a total of 31 endometrioid adenocarcinomas with paired DNA (tumor and normal) by SNP arrays (25 samples on the Affymetrix 50K array and 6 on the 250K array). Chromosomal imbalances with one or more loci were detected in 26 (84%) out of 31 tumors. Gains on chromosome arms were observed on 1q (29%), 2p (10%), 7q (13%), 8p (10%), 8q (19%), 10p (10%), 10q (13%), 12p (16%), 12q (16%), 17q (10%), 20p (13%) and 20q (10%). LOH was detected on 1p (19%), 1q (10%), 2q (13%), 5q (13%), 6q (19%), 9p (16%), 9q (16%), 10q (29%), 16q (19%), 17p (16%) and 22p (10%) (Figure 1 and Supplementary Table 2). The regions of these gains and losses were compatible with the reports by comparative genomic hybridization (CGH) (Suehiro *et al.*, 2000; Micci *et al.*, 2004; Levan *et al.*, 2006).

CNN LOH involves allelic changes, including hemizygous deletion with a gain of the opposite allele. In addition to chromosomal gains (16/31; 52%) and LOH (19/31; 61%), we detected CNN LOH in 13 samples (42%) at 54 regions (Table 1). All these CNN LOH are somatic events, as these regions in the tumors were identified by retention of heterozygsity in the paired germline DNA. In addition, we assessed known copy number variations (CNVs) from the Database of Genomic Variants v8 (http://projects.tcag.ca/variation/), and confirmed that all of these 54 CNN LOH included non-CNV regions. The regions of CNN LOH include 8q and 10q, at which copy number gains are frequently detected in endometrial carcinomas. Five of the 54 CNN LOH (9%) occur in the whole arm of each chromosome (1p, 1q, 6p, 18p and 18q). The minimal CNN LOH region in 51 out of the 54 was more than 100 kb, and the other three regions with <100 kb were detected in both the 50K and the 250K SNP array (Table 1), suggesting that the 50K SNP probes distinguish CNN LOH at a comparable level with the 250K probes. We found that the CNN LOH regions frequently include the loci of several well-known tumor suppressor genes, such as *CDKN2A* (9p21.3), *PTEN* (10q23.3) and *TP53* (17p13.1).

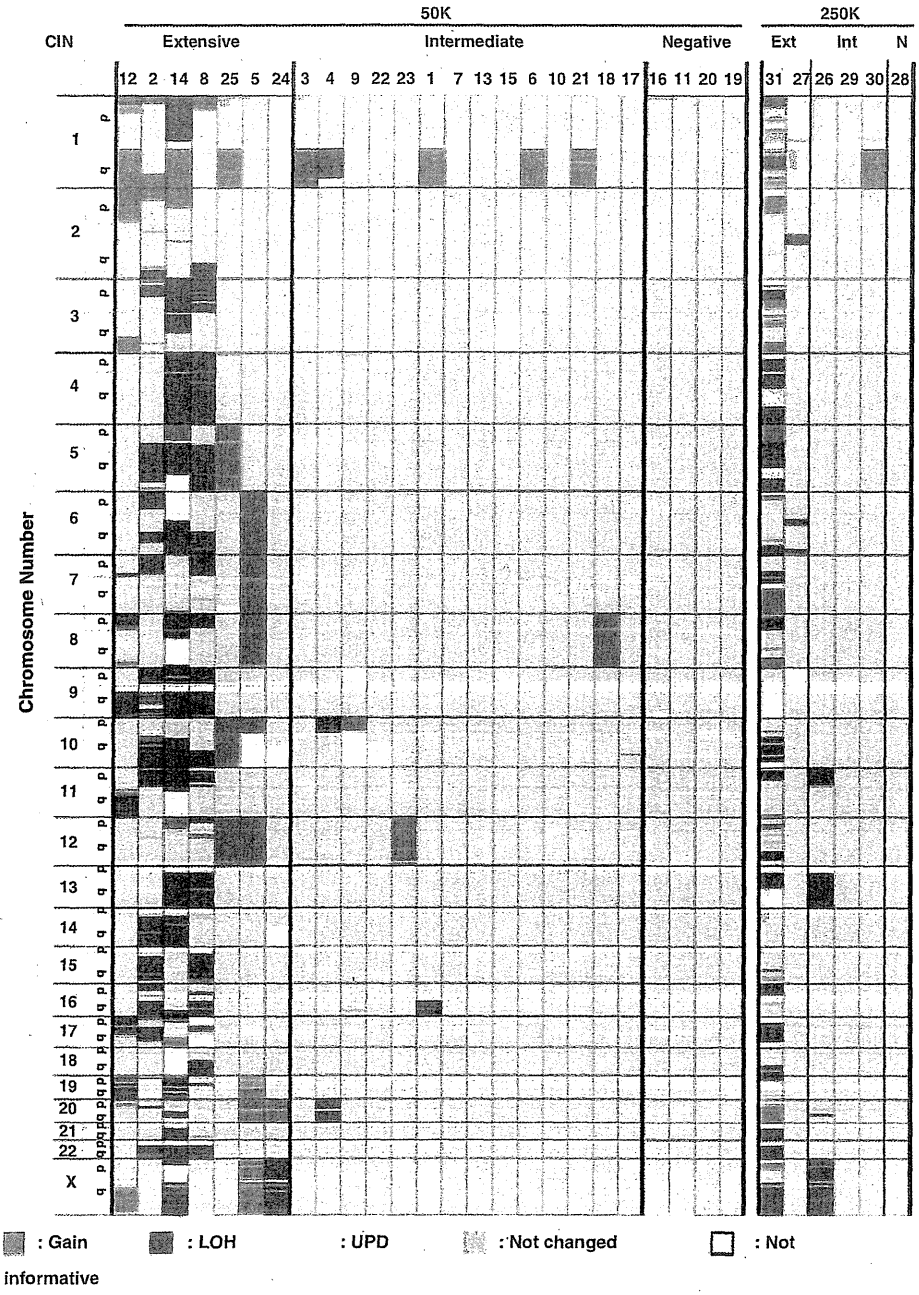

Figure 1 Overview of genomic imbalance in endometrial carcinomas. SNP array was performed in 31 clinical samples with paired tumor DNA and normal DNA, using a human mapping 50K or 250K Array. Samples are categorized according to the level of chromosomal instability (CIN) as described in the text; CIN-extensive (Ext) with five or more copy number changes, CIN-intermediate (Int) with 1–4 copy number changes, and CIN-negative (N) without any copy number changes.

We detected five HD candidate regions in three samples. One of the five regions (6q21.2) was located in the vicinity of a known CNV. Genome imbalance map (GIM) algorithm using the control DNA in this sample with the other from unrelated individuals revealed hemizygous loss at the surrounding region in the germline DNA, suggesting that this locus is not somatic HD. The other four HD regions on 9p21.3, 10q23.3, 11p15.1 and 17q11.21 did not match with any known CNVs and included *CDKN2A*, *CDKN2B*, *ELAVL2*, *PTEN*, *NELL1*, *IDH3GL* and *NF1* genes. All these regions were <4.2 Mb and were included in the LOH regions (Figure 1 and Supplementary Table 3).

SNP array genotyping distinguishes three clusters according to the degree of CIN

As the number of copy alterations is significantly different in each tumor, we further divided the CIN-positive tumors into CIN-extensive and CIN-intermedi-

Table 1 Minimal regions of copy number neutral (CNN) LOH in endometrial carcinomas

SNP probes	*Sample#*	*Chromosome/ cytoband*	*Start*	*End*	*Minimal region (Mb)*	*Cancer-related genes*
	1	1p36.32–1p36.11	3 464 664	24 689 967	21.225303	*MDS2, SDHB, PAX7, RPL22*
	2	11p13	34 400 995	34 569 744	0.168749	
		14q24.1	66 751 027	67 553 008	0.801981	*RAD51L1*
	5	10q11.23–10q26.3*	49 154 970	132 221 295	83.066325	*BMPR1A, NCOA, D10S170, LCX, PRF1, MYST4, PTEN, NFKB2, TLX1, TNFRSF6, SUFU, FGFR2*
	8	3p14.2–3p14.1	61 464 727	64 834 115	3.369388	
		6q23.2	134 231 263	134 325 485	0.094222	
		7p15.2	25 504 107	25 728 845	0.224738	
		9p22.3	15 722 332	15 750 822	0.02849	
		11p15.4	2 861 092	8 302 275	5.441183	*LMO1, NUP98*
		12q13.13	50 605 518	51 445 539	0.840021	
		17p13.3–17p11.2	489 977	22 269 537	21.77956	*GAS7, BHD, HCMOGT-1, MAP2K4, RAB5EP, TP53, USP6*
		17q21.31–17q21.32	42 127 241	46 355 386	4.228145	
		17q21.33–17q25.3	48 767 363	81 267 388	32.500025	*DDX5, BRIP1, HLF, MSI2, PRKAR1A, ASPSCR1, CANT1, ALO17, MSF*
	9	3q26.31–3q29	176 959 377	198 389 829	21.430452	*PIK3CA, BCL6, EIF4A2, ETV5, LPP, TFRC*
		9p24.3–9p13.3	239 391	35 436 386	35.196995	*FANCG, CDKN2A- p14ARF, CDKN2A -p16(INK4a), MLLT3, PSIP2, JAK2*
50K		10q11.21–10q26.3*	43 685 003	134 750 136	91.065133	*BMPR1A, NCOA4, D10S170, LCX, PRF1, MYST4, PTEN, NFKB2, TLX1, TNFRSF6, SUFU, FGFR2*
	10	3p26.3–3p21.33	394 143	43 747 869	43.353726	*PPARG, MLH1, CTNNB1, RAF1, VHL, XPC, SRGAP3, FANCD2*
	14	5q31.1–5q35.3	135 051 159	180 180 911	45.129752	*GRAF, ITK, PDGFRB, CD74, RANBP17, NPM1, NSD1, TLX3*
		6p	Whole arm	Whole arm	Whole arm	*HSPCB, CCND3, HMGA1, SFRS3, TFEB, PIM1, HIST1H4I, POU5F1, FANCE, TRIM27, DEK*
		6q11.1–6q14.1	62 019 084	78 728 757	16.709673	
		8q13.1–8q24.23	67 274 844	137 516 772	70.241928	*NCOA2, NBS1, CBFA2T1, COX6C, EXT1, MYC*
		11q13.1–11q25	64 820 346	134 034 111	69.213765	*NUMA1, CCND1, PICALM, ATM, BIRC3, MAML2, DDX10, PAFAH1B2, MLL, SDHD, POU2AF1, ZNF145, CBL, DDX6, PCSK7, ARHGEF12, FLI1*
		18p	Whole arm	Whole arm	Whole arm	
		18q	Whole arm	Whole arm	Whole arm	*SS18, ZNF521, MALT1, MADH4, FVT1, BCL2*
		20q13.13–20q13.33	50 442 828	62 317 398	11.87457	*GNAS, SS18L1*
		Xp22.13–Xp11.22	18 593 051	49 297 523	30.704472	*TFE3, SSX4, GATA1, SSX1 , WAS*
	15	3q12.1–3q29	99 594 845	197 114 668	97.519823	*MDS1, TFG, CBLB, ZNF9, GATA2, RPN1, FOXL2, GMPS, MLF1, EVI1, PIK3CA, BCL6, EIF4A2, ETV5, LPP, TFRC*
	22	10q22.2–10q26.3*	75 028 193	132 221 295	57.193102	*BMPR1A, MYST4, PTEN, NFKB2, TLX1, TNFRSF6, SUFU, FGFR2*
	24	1p	Whole arm	Whole arm	Whole arm	*RBM15, TRIM33, NRAS, NOTCH2, BCL10, SIL, EPS15, TAL1, SFPQ,THRAP3, MYCL1, MUTYH, LCK,MDS2, SDHB,PRDM16, PAX7, RPL22, MPL*
		1q	Whole arm	Whole arm	Whole arm	*PDE4DIP, BCL9, IRTA1, MUC1, AF1Q, ARNT, SDHC, PRCC, NTRK1, HRPT2, TPM3, FCGR2B, PBX1, PMX1, ABL2, TPR, ELK4, MDM4, SLC45A3, FH*
		10q22.2–10q26.3*	74 940 617	134 813 136	59.872519	*BMPR1A, MYST4, PTEN, NFKB2, TLX1, TNFRSF6, SUFU, FGFR2*
		14q22.3–14q32.33	53 559 881	102 230 659	48.670778	*KTN1, RAD51L1, GPHN*
	27	1p36.33–1p13.2	1 308 770	114 590 824	113.282054	*BCL10, SIL, EPS15, TAL1, SFPQ, THRAP3, MYCL1, MUTYH, LCK, MDS2, SDHB, PRDM16, PAX7, RPL22*
		9p24.3–9p13.3	264 108	35 051 504	34.787396	*CDKN2A- p14ARF, CDKN2A -p16(INK4a), MLLT3, PSIP2, JAK2*
	29	2p25.3–2p12	124 249	82 139 344	82.015095	*REL, IGK@,BCL11A, MSH6, EML4, MSH2, NCOA1, ALK, MYCN*
	31	1p35.2–1p31.2	30 984 284	59 013 240	28.028956	*SIL, EPS15, TAL1, SFPQ,THRAP3, MYCL1, MUTYH, LCK*
		1q23.2	156 672 464	157 185 184	0.51272	
		3p26.3–3p24.3	79 972	18 006 232	17.92626	*PPARG, RAF1, VHL, XPC, SRGAP3, FANCD2*
		3p24.3–3p24.1	20 755 592	29 221 196	8.465604	
		4p16.3–4p1533	344 051	14 519 067	14.175016	*WHSC1, FGFR3*
		4q22.3–4q31.21	94 588 552	143 180 768	48.592216	*TET2, IL2*
		4q31.23	149 715 072	149 730 992	0.01592	
250K		5q21.1	99 140 632	99 692 424	0.551792	
		5q23.1–5q32	117 033 848	146 035 968	29.00212	
		6p25.3–6p24.3	119 769	8 827 918	8.708149	*IRF4*

Table 1 Continued

SNP probes	*Sample#*	*Chromosome/ cytoband*	*Start*	*End*	*Minimal region (Mb)*	*Cancer-related genes*
		7q11.23–7q21.2	75 341 256	90 787 048	15.445792	
		8p23.2–8p21.1	198 834	6 508 840	6.310006	
		9q21.11–9q34.3	68 854 248	138 262 432	69.408184	*GNAQ, SYK, NR4A3, FANCC, PTCH, XPA, OMD, FNBP1, TAL2, CEP1, BRD3, SET, TSC1, NUP214, ABL1*
		10q25.3–10q26.3	117 468 544	135 293 424	17.82488	*FGFR2*
		13q21.2–13q34	60 518 320	114 054 472	53.536152	*ERCC5*
		17p13.1–17p12	83 173	14 791 705	14.708532	*RAB5EP, TP53, USP6, PER1*
		17q24.3–17q25.3	66 106 416	78 531 856	12.42544	*ASPSCR1, CANT1, ALO17*
		20p13–20p12.1	165 074	15 279 007	15.113933	
		21q21.2–21q21.3	25 499 006	26 046 936	0.54793	

Abbreviation: SNP, single-nucleotide polymorphism.
*Regions including the locus of PTEN.

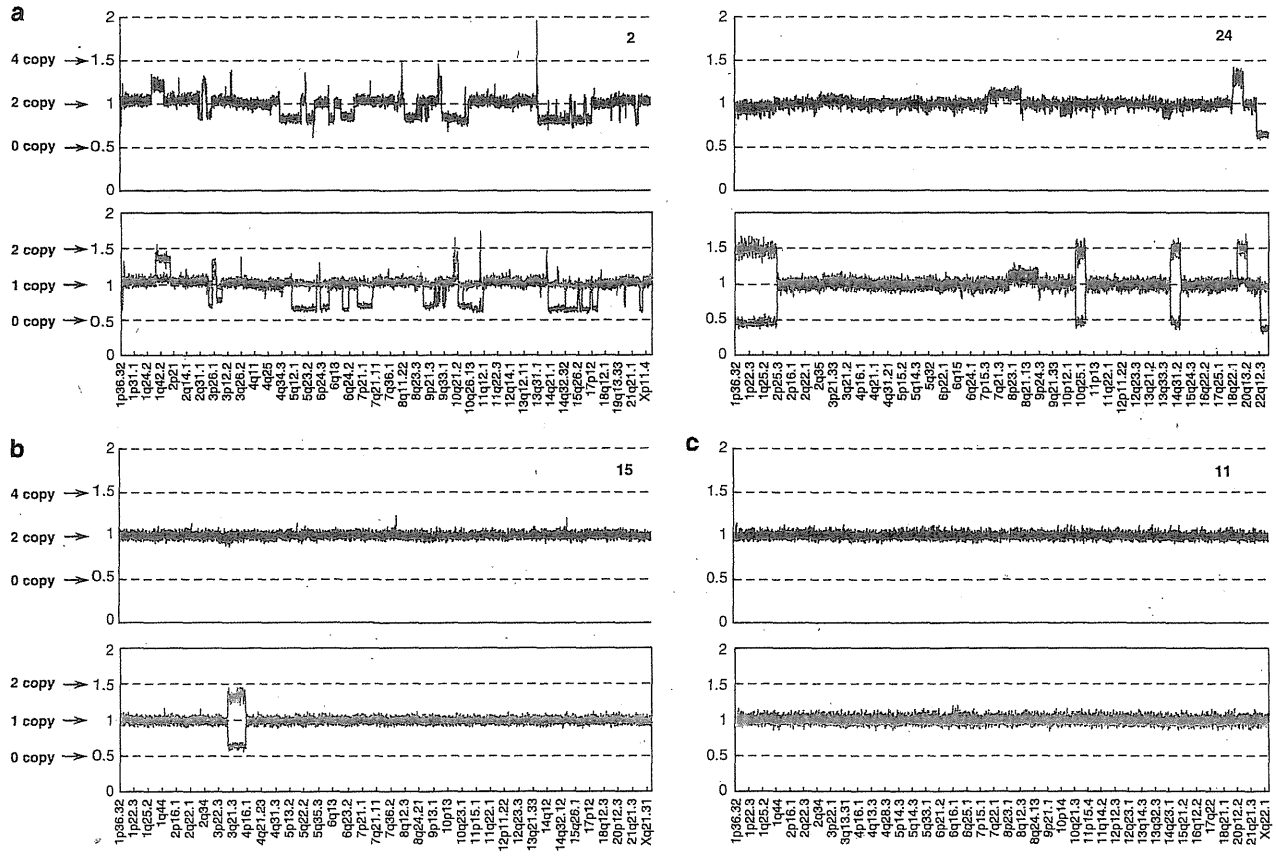

Figure 2 SNP array 'karyograms' (50K) of representative tumors. In each graph, the top shows the total copy number and the bottom shows the allele-specific copy number. CIN status is classified according to the number of loci with chromosomal imbalances. (**a**) Karyograms of two CIN-extensive tumors. CNN LOHs are predominantly detected in one sample at1p, 1q, 10q22.2–26.3 and 14q22–32 (*right*). (**b**) Karyogram of one CIN-intermediate tumor. (**c**) Karyogram of one CIN-negative tumor.

ate. The SNP array 'karyograms' of representative tumors are shown in Figure 2. We classified tumors with five or more loci of copy alterations as CIN-extensive (Figure 2a), those with one to four loci as CIN-intermediate (Figure 2b), and those without any copy alterations as CIN-negative (Figure 2c). The karyograms of the remaining tumors are available in Supplementary Figure 1. In this classification, 9 out of 31 (29%) tumors were CIN-extensive, 17 (55%) were CIN-intermediate and 5 (16%) were CIN-negative (Figure 1). Whole arm chromosomal alterations were more frequently observed in CIN-extensive than in CIN-intermediate tumors (Figure 1 and Supplementary Figure 1).

Table 2 Status of microsatellite instability (MSI) and chromosomal instability (CIN)

	No.	*D2S123*	*D5S346*	*D17S250*	*BAT25*	*BAT26*	*CIN*
	24	+	+	+	+	+	Ext
	6	+	+	+	+	+	Int
	10	+	+	+	+	+	Int
	15	+	−	+	+	+	Int
MSI-high	17	+	+	+	+	+	Int
	18	+	+	+	+	+	Int
	21	+	+	−	+	−	Int
	11	−	+	+	+	+	Neg
	19	+	−	−	+	+	Neg
	20	+	−	+	+	+	Neg
	2	−	−	−	−	−	Ext
	5	−	−	−	−	−	Ext
	8	−	−	NA	−	−	Ext
	12	−	−	−	−	−	Ext
	14	−	−	−	−	−	Ext
	25	−	−	−	−	−	Ext
	1	−	−	−	−	−	Int
MSS	3	−	−	−	−	−	Int
	4	−	−	−	−	−	Int
	7	−	−	−	−	−	Int
	9	−	−	−	−	−	Int
	13	−	−	−	−	−	Int
	22	−	−	−	−	−	Int
	23	−	−	−	−	−	Int
	16	−	−	−	−	−	Neg

Abbreviations: Ext, extensive; Int, intermediate; MSS, microsatellite stable; NA, not available; Neg, negative.

MSI-high is commonly coexistent with CIN-negative and CIN-intermediate, but rarely with CIN-extensive

In this study, MSI-high was detected in 10 out of 25 (40%) endometrial carcinomas, and microsatellite stable (MSS) in 15 out of 25 (60%) (Table 2). MSI-low was not detected in this study. MSI-high was detected in 1 of 7 (14%) in CIN-extensive, 6 of 14 (43%) in CIN-intermediate and 3 of 4 (75%) in CIN-negative tumors, suggesting an inverse correlation between CIN and MSI. As a result, 24 of 25 (96%) endometrial carcinomas were positive for genomic instability (MSI and/or CIN).

We analyzed the clinicopathological characteristics of CIN-extensive. No significant difference in age, differentiation, vascular invasion, clinical stage and myometrial invasion was observed between CIN-extensive and the others (Supplementary Table 4). Presence of CNN LOH also does not have any significant associations in these factors (data not shown). MSI-high was correlated with vascular invasion ($P=0.049$), and shows a tendency toward unfavorable clinicopathological features, such as deep myometrial invasion and old age (Supplementary Table 5).

CIN-extensive is a poor prognostic factor in endometrial carcinomas

By Kaplan–Meier analysis, MSI-high showed a trend to be a favorable prognostic factor ($P=0.069$) (Supplementary Figure 2a). Next, we analyzed 50K SNP array in the other 11 endometrial carcinomas using tumor DNA, in addition to the 31 tumors. In 42 tumors, the ratio of CIN-extensive, -intermediate and -negative is 26% (11/42), 52% (22/42) and 21% (9/42), respectively. Kaplan–Meier analysis revealed that CIN-extensive was a significant marker of poor prognosis ($P=0.0034$ by log-rank test, Figure 3). A worse prognosis of CIN-extensive, compared with CIN-intermediate ($P=0.0033$, Supplementary Figure 2b), suggests that not only the existence but also the degree of CIN is important in endometrial tumorigenesis. Stage III–IV and histological grade (grade 2 or 3) were also poor prognostic factors by univariate analysis (Table 3). Subsequently, multivariate analysis was conducted using these three poor prognostic factors. Only CIN-extensive was found to be a significant and independent predictor for poor survival (Table 3).

Frequent CNN LOH with homozygous PTEN *mutations in endometrial carcinomas*

In SNP array analysis, we detected deletions of *PTEN* locus in 8 out of 31 (26%) tumors: one with HD, four with CNN LOH (marked with an asterisk in Table 1) and three with LOH without gain of the opposite allele. We also evaluated *PTEN* mutations and detected the mutations in 16 of 22 (73%) tumors. Taken together, we found three patterns of biallelic *PTEN* alterations in a total of eight tumors (36%): three tumors with CNN LOH and a mutation, four with two mutations and one with HD (Supplementary Table 6). Monoallelic *PTEN* alterations were observed in 11 tumors (50%): nine with a mutation, one with CNN LOH and one with LOH (Supplementary Table 6). Only three (14%) tumors showed no genomic alterations in *PTEN*. In our previous study, we did not observe any *PTEN* hypermethylation in 53 endometrial carcinomas (Shoji *et al.*, 2009).

MSS tumors frequently possess chromosomal imbalances in genes associated with the Ras-PI3K pathway

MSI is thought to correlate with mutator phenotype, and is reported to possess *PTEN* mutations more frequently than MSS in endometrial carcinomas. Indeed, all the MSI-high tumors possess *PTEN* mutations, whereas 6 of 12 MSS tumors (50%) possess *PTEN* mutations ($P=0.015$) (Supplementary Table 6). On the other hand, we found that six out of seven (87%) tumors with chromosomal imbalances of *PTEN* were MSS, suggesting that chromosomal imbalances have significant roles in disrupting PTEN function in MSS tumors.

Next, we analyzed genomic alterations of the other Ras-PI3K-related genes (*NF1*, *K-Ras* and *PIK3CA*). We found mutations of *K-Ras* and *PIK3CA* in 2 (9%) and 6 (27%) out of 22 tumors, respectively. In addition to one HD (4%) and two LOH (8%) at the *NF1* locus, we found gains at the loci of *PIK3CA* (3q26.3) in four (16%) tumors and *K-Ras* (12p12.1) in four (16%) tumors. CNN LOH at the loci of *PIK3CA* was observed in two (8%) tumors, including one with a *PIK3CA* mutation.

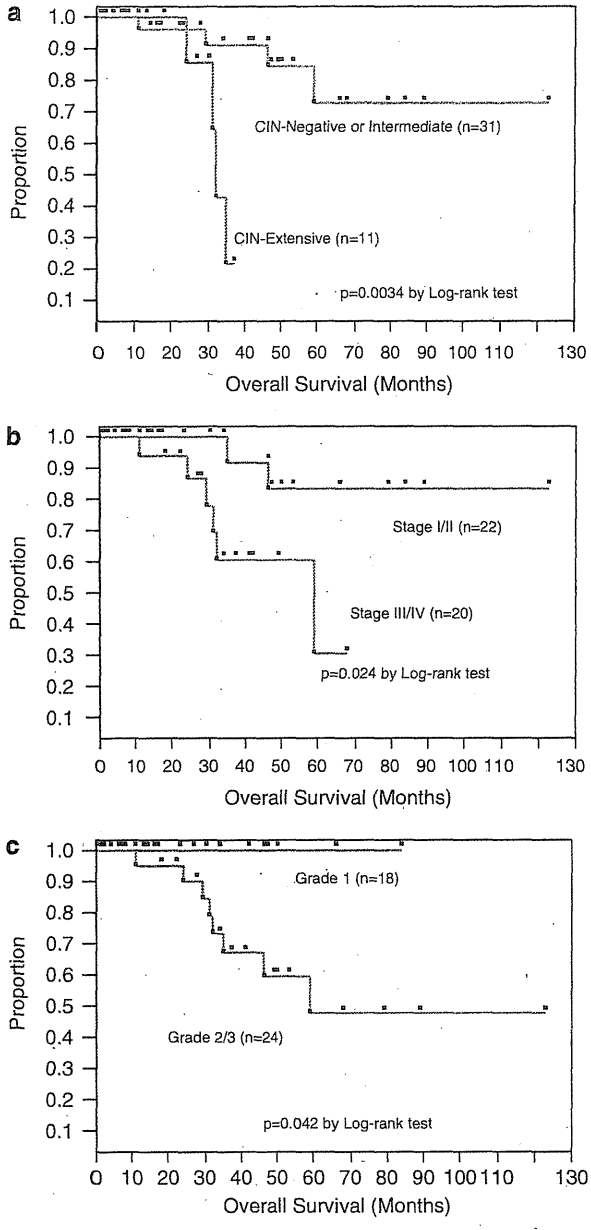

Figure 3 Overall survival of 42 endometrial carcinomas calculated according to the Kaplan–Meier method. (**a**) Survival of patients with CIN-extensive ($n=11$), compared with the others (CIN-negative or -intermediate ($n=31$). (**b**) Survival of stage III–IV patients ($n=20$) compared with stage I–II patients ($n=22$). (**c**) Survival of patients with histological grade 2–3 ($n=24$), compared with those with grade 1 ($n=18$).

We summarized the data of genomic alterations in the four genes (*PTEN*, *PIK3CA*, *K-Ras* and *NF1*) of the Ras-PI3K pathway (Table 4). In total, six out of the seven CIN-extensive tumors show deletion(s) in *PTEN* and/or *NF1*. Although the biological functions of copy number gains in *K-Ras* and *PIK3CA* are to be elucidated, all the seven CIN-extensive tumors show chromosomal imbalances in the loci of genes associated with the Ras-PI3K pathway, whereas 5 of the 14 CIN-intermediate tumors (36%) show such imbalances

Table 3 Univariate and multivariate analysis of prognostic factors for

Prognostic factor	P	
	Univariate	*Multivariate*
Age >60 (vs −60)	0.57	
Grade 2/3 (vs grade 1)	0.0099	0.070
FIGO stage III/IV (vs I/II)	0.026	0.27
Myometrial invasion >2/3 (vs <2/3)	0.62	
CIN-extensive (vs others)	0.011	0.048

Abbreviation: CIN, chromosomal instability.

($P=0.016$) (Table 4). In total, genetic mutations in the Ras-PI3K pathway and/or copy number losses in *PTEN* and/or *NF1* were detected in 20 of 22 tumors (91%). The 250K SNP array also revealed LOH in both *PTEN* and *NF1* genes in one of the six tumors.

Discussion

The relationship between CIN and MSI in endometrial carcinomas

Our analyses of genomic instability revealed that most of the endometrial carcinomas possess CIN and/or MSI. The positive ratios of CIN and MSI were 84% (21/25) and 40% (10/25), respectively. Inconsistent with colorectal cancer (Choi *et al.*, 2002), coexistence of MSI-high and positive CIN was observed in 28% (7/25) of our samples, especially in CIN-intermediate tumors (6/14=43%). This overlap might be explained, at least in part, by the detection of CNN LOH, as described below. The ratio of MSI-high (40%) in this study was higher than that (15–20%) in previous reports (Atkin, 2001; Woerner *et al.*, 2003), presumably because all the tumors in this study are endometrioid adenocarcinomas. In spite of correlation with lymphovascular invasion, MSI-high showed a trend of favorable prognosis. Positive MSI was also reported to correlate with advanced stage and deep myometrial invasion in endometrial carcinomas (Black *et al.*, 2006). On the other hand, we showed that CIN-extensive was an independent poor prognostic factor, without any significant associations with clinicopathological factors. These data suggest that the aggressive phenotype of CIN-extensive tumors is not predicted by any clinicopathological characteristics, and the favorable prognosis in MSI-high tumors might be explained by the inverse trend between MSI and CIN status. In this analysis, we added SNP array data from 11 specimens with only tumor DNA, in addition to 31 specimens with both tumor and normal DNA. We confirmed that the presence of CNN LOH affected the classification (CIN-extensive versus others) only in one of the 31 specimens with paired DNA. An additional 10 specimens classified by array CGH also supported the poor prognostic effect of CIN-extensive (data not shown). Therefore, our CIN classification would be also applicable to the data of either SNP array without normal DNA or array CGH. Although the SNP typing

Table 4 Mutations and copy number (CN) imbalances in Ras-PI3K pathway

CIN	*MSI*	*Number of genes with alterations*		*Types of alterations*					*Sample*
		Mutations	*CN imbalances*	*PTEN*	*Mutated codon(s)*	*PIK3CA*	*K-Ras*	*NF1*	
Negative									
1	High	2		Mut + Mut	(R173C/P213H)	Mut (D549N/T1025A)			19
2	High	1		Mut	(K164R)				11
3	High	1		Mut	(318-319; Del CTTA)				20
4	Negative	1		Mut	(L25F)				16
Intermediate									
1	High	3		Mut + Mut	(100; Ins A/291-293; Del 7bp)	Mut (H1047R)	Mut (G12C)		6
2	High	2	1	Mut + Mut	(164; Del A/268; Del A)	Mut (H1047R) + CNN LOH			15
3	High	2		Mut	(232; Ins A)	Mut (E542 K)			10
4	High	2		Mut	(274; Del T)	Mut (H1047Y)			18
5	High	2		Mut	(137; Del A)		Mut (G13D)		21
6	High	1		Mut	(R173C)				17
7	Negative	2		Mut	(13; Ins C)	Mut (N1044 K)			13
8	Negative	1		Mut + Mut	(R130G/R233*(stop))				4
9	Negative	1	2	Mut + CNN LOH	(291; Ins A)	CNN LOH			9
10	Negative	1	1	Mut	(L146*(stop))		Gain		23
11	Negative		1	CNN LOH					22
12	Negative								3
13	Negative	NA	1	NA		Gain			1
14	Negative	NA		NA					7
Extensive									
1	High	1	1	Mut + CNN LOH	(G132R)				24
2	Negative	1	1	Mut + CNN LOH	(R130G)				5
3	Negative		3	HD		Gain		HD	2
4	Negative		3	LOH		Gain	Gain	LOH	8
5	Negative		2			Gain		LOH	12
6	Negative		1				Gain		25
7	Negative	NA	2	LOH			Gain		14

Abbreviations: HD, homozygous deletion; PI3K, phosphatidylinositol 3′-kinase.

array or array CGH may not be currently cost-effective, defining CIN status will become more feasible with the prevalence of genome-wide analysis of each cancer. The information that all the patients with risk factors (such as lymph node metastasis and deep myometrial invasion) received adjuvant radiation and/or chemotherapy suggests that CIN-extensive might be also associated with sensitivity to adjuvant chemotherapy and/or radiotherapy. The loci of copy alterations in CIN-extensive did not frequently overlap with each other in our analyses (Figure 1). Rather, the region of copy alterations spreads to the entire genome. The numerous patterns of copy alterations in CIN-extensive tumors indicate that the degree of CIN itself, not the alterations of specific genes, might be a significant marker for tumor aggressiveness.

CNN LOH and HD in endometrial carcinomas

Recently, CNN LOH has been reported in various types of tumors at the loci of important genes that drive the carcinogenic process (Bacolod *et al.*, 2009; Tuna *et al.*, 2009). The ratio of CNN LOH was reported at 20–50% in several tumors, including leukemia, liver cancer and ovarian cancer (Raghavan *et al.*, 2005; Midorikawa *et al.*, 2006; Dunbar *et al.*, 2008; Walsh *et al.*, 2008). Considering the fact that only 28% of tumors were CIN-extensive, it is noteworthy that CNN LOH was positive in 42% of endometrial carcinomas. Especially, 3 of 14 CIN-intermediate tumors show CNN LOH alone without any other chromosomal gains and losses that would be overlooked by CGH. These results suggest that CNN LOH shares a significant ratio and may have key roles in endometrial carcinogenesis. We found one HD and one CNN LOH at the *CDKN2A* locus (9p21.3) and two CNN LOH at the *TP53* locus (17p13.1). These alterations have been reported in other types of malignancy such as of the colon, breast and leukocyte (Melcher *et al.*, 2007; Kawamata *et al.*, 2008; Walsh *et al.*, 2008). In gynecologic malignancies, HD at 9p21.3, 10q23.3, 17q11.2 and CNN LOH at 1p36.13–1p36.11, 13q31.1, 13q32.3–13q34, 17p13.2–17p11.2, 17q21.33–17q23.2, Xp21.1 and Xp11.4–Xp11.3 were also reported in ovarian cancer (Gorringe *et al.*, 2009). Thus, CNN

LOH and HD of specific tumor suppressor genes might be widespread in various types of tumors.

Copy number polymorphisms are known to be common in the human genome (Conrad *et al.*, 2006). Normalization of tumor samples to their matching normal germline DNA is a useful method to mask such copy number polymorphisms; however, copy number polymorphisms and interchromosomal segmental duplications can still masquerade as somatic alterations in tumors with extensive copy number imbalances (Gorringe and Campbell, 2008). In our analysis, one HD at 6q21.2 was suggested to be one of the germline CNVs. Thus, it is very important to exclude the possibility of germline CNVs in each HD region.

Biallelic PTEN inactivation and MSI status

The most frequent CNN LOH was 10q22.2–10q26.3, which includes *PTEN*. The ratio of LOH in *PTEN* has been reported to be 20–40% by microsatellite markers and approximately 15% by CGH (Sirchia *et al.*, 2000; Suehiro *et al.*, 2000; Toda *et al.*, 2001; Micci *et al.*, 2004; Levan *et al.*, 2006). In our analysis, four of seven LOH detected at the *PTEN* locus turned out to be CNN LOH, indicating that LOH of *PTEN* has been underestimated by CGH in endometrial carcinomas. Three of the four tumors with CNN LOH at *PTEN* possess homozygous *PTEN* mutations. In addition, HD of *PTEN* at 10q23 was also detected in one tumor. We previously reported multiple *PTEN* mutations in 9 out of 37 *PTEN* mutant tumors (Minaguchi *et al.*, 2001). Taken together, inactivation of *PTEN* is caused by various reasons, such as (1) a mutation and LOH without gain of the opposite allele, (2) homozygous mutations and CNN LOH, (3) HD and (4) mutations in both alleles. There might be other unknown mechanisms of biallelic *PTEN* inactivation, as 11 tumors showed monoallelic *PTEN* alterations in this study, including one tumor with CNN LOH at *PTEN*. *PTEN* mutations in endometrial carcinomas were reported to be more common in MSI-positive tumors, compared with MSS tumors (Bilbao *et al.*, 2006). In this study, all the three tumors with multiple *PTEN* mutations were MSI-high, whereas six out of seven tumors with *PTEN* deletion(s) were MSS. These data suggest that the mechanism of *PTEN* inactivation is affected by MSI status.

Prevalent genomic alterations in the Ras signaling pathway

The frequency of mutations in *K-Ras*, *PTEN* and *PIK3CA* in the Ras-PI3K pathway is remarkable in endometrial carcinomas. *NF1*, located at 17q11.2, functions as a negative regulator of the Ras signaling pathway (McCormick, 1995). Recently, CNN LOH surrounding the *NF1* locus was observed in juvenile myelomonocytic leukemia (Flotho *et al.*, 2007). Although inactivation of *NF1* has not been reported in endometrial carcinomas, we have detected one HD at 17q11.2 and three LOH at this locus in 31 samples (13%). Copy number losses in *NF1* suggest that there might be other types of alterations in this gene in endometrial carcinomas, such as inactivating mutations reported in glioblastomas (Cancer Genome Atlas Research Network, 2008).

Amplifications of *PIK3CA* (3q26.3) and *K-Ras* (12p12.1) loci are other possible mechanisms of alterations. SNP array analysis revealed copy number gains at the locus of *K-Ras* (13%) and *PIK3CA* (13%), supporting the previous reports (Oda *et al.*, 2005; Salvesen *et al.*, 2009). One of the two tumors with CNN LOH at the *PIK3CA* locus contains a 'hot spot' *PIK3CA* mutation (H1047R), which might result in increased activity of mutant p110alpha. However, it is to be elucidated whether gains (and CNN LOH without a mutation in the opposite allele) at the loci of *PIK3CA* and *K-Ras* are in fact targeting these genes. Comprehensive analyses of genomic alterations in the Ras-PI3K pathway revealed that genomic alterations in the Ras-PI3K pathway are extensively common, as observed in Table 4. These results suggest that the activation of this pathway might be a critical step in endometrial tumorigenesis and that targeting this pathway might be a promising therapeutic strategy in endometrial carcinomas.

Materials and methods

Tumor samples and genomic DNA

Surgical samples were obtained from a total of 42 patients with primary endometrial carcinomas (endometrioid adenocarcinomas) who underwent resection of their tumors at the University of Tokyo Hospital. All the 42 patients were treated as previously described (Onda *et al.*, 1997). Briefly, they received primary surgery, including hysterectomy, bilateral salpingo-oophorectomy and systematic lymphadenectomy. Whole-pelvis irradiation was indicated for stage I–III patients with at least one of the following factors: deep myometrial invasion, positive lymph nodes, adnexal metastases and pelvic peritoneal metastases. The stage III patients with either adnexal/peritoneal involvement or aortic node metastases were treated with three cycles of platinum-based chemotherapy before radiation therapy. Stage IV patients were treated postoperatively with five cycles of platinum-based chemotherapy. All the recurrent patients received platinum-based chemotherapy.

All of the patients provided informed consent for the research use of their samples and the collection, and the use of tissues for this study was approved by the appropriate institutional ethics committees. The fresh-frozen tumors were embedded in OCT compound, and the 4-μm tissue sections were stained with hematoxylin and eosin. We confirmed that each section contains a high purity of tumor epithelium (>60%) and used those sections for DNA extraction. Genomic DNA was isolated from the tumor sections or lymphocyte pellets using a QIAamp DNA Mini Kit (Qiagen, Valencia, CA, USA), according to the manufacturer's specifications. Paired genomic DNA was also extracted as a control through blood samples in 31 out of 42 patients. The clinical status of these 42 patients was summarized in Supplementary Table 1.

SNP array

SNP array was performed in 31 clinical samples with paired tumor DNA and normal DNA, and 11 clinical samples with tumor DNA alone. Experimental procedures for GeneChip

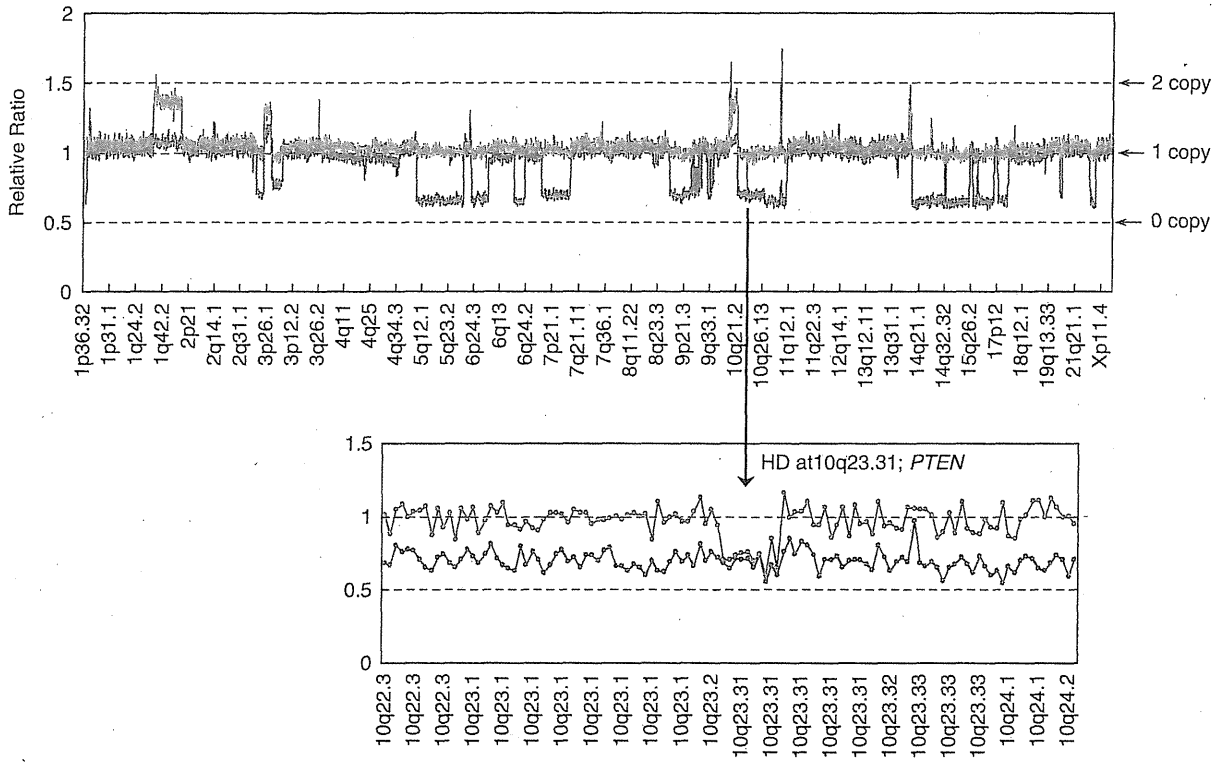

Figure 4 Detection of allele-specific copy number alterations, including homozygous deletions (HD), using a human mapping 50K SNP array technology. Red bar corresponds to the allele with a higher copy number, and blue bar to that with a lower copy number. This representative sample shows LOH at multiple loci (top). Inside the LOH, chromosome 10q23.3 is homozygously deleted as shown in the bottom.

were performed according to GeneChip Expression Analysis Technical Manual (Affymetrix, Santa Clara, CA, USA), using a Human mapping 50K Xba I Array in 36 out of 42 samples. The remaining six samples with paired DNA were analyzed with a Human mapping 250K Nsp Array (Affymetrix).

Genome imbalance map

The GIM algorithm was applied to the raw data of endometrial cancer and peripheral blood obtained from SNP arrays. We previously reported that the purity of tumor epithelium at 50% is sufficient for the GIM algorithm (Ishikawa *et al*., 2005). The basic concept of GIM involves the normalization of probe level signals, as previously described (Ishikawa *et al*., 2005). Briefly, the signal intensity ratio between the raw signal intensity from the cancer and paired normal samples was calculated from the perfect match probes for each SNP locus by taking the median after omitting the highest and lowest values. Second, we calculated the adjusted ratio, which is the raw ratio divided by the expected ratio. The expected ratio is calculated by adjusting several parameters for each experiment, for example, length of *Xba* I (or Nsp) fragment, percentage of GC of *Xba* I (or Nsp) fragments, local GC content, hybridization-free energy of 25-mer probe sequences and genomic mean of signal intensity of perfect match probes from reference sample. For allele-specific copy number analysis in this GIM algorism, the relative ratio of 0.5, 1 and 1.5 theoretically corresponds to 0, 1 and 2 copies, respectively (Figure 4). We detected allele-specific copy number alterations, using the cutoff relative ratio of >1.3 (1.6 copies) for gain and <0.7 (0.4 copies) for loss in each region. Total copy number alterations were also detected by using the cutoff relative ratio of >1.15 (2.6 copies) for gain and <0.85 (1.4 copies) for loss.

MSI analysis

Genomic DNAs extracted from the samples were used to study MSI status using five fluorescence-labeled microsatellite markers (BAT25, BAT26, D2S123, D5S346 and D17S250). Primer sequences have been previously described (Loukola *et al*., 2001). PCR reactions were performed with KOD plus DNA Polymerase (TOYOBO, Osaka, Japan). The PCR conditions were as follows: 94°C for 2 min; 30 cycles of 94°C for 15 s, 54–60°C for 30 s, 68°C for 30 s, followed by a final extension at 68°C for 2 min. After PCR, 1 μl of the product ($\times 30$ diluted) was mixed with 10 μl Hi-di Formamide and a size marker. This product was denatured at 95°C for 5 min and cooled on ice before loading onto ABI 3130 Genetic Analyzer (Applied Biosystems, Foster City, CA, USA). Results were analyzed by Genemapper Software Version 4.0 (Applied Biosystems). Determination of MSI status was made according to the presence of mutant alleles in tumor DNA compared with blood DNA. MSI status was determined as follows: tumors with two or more positive MSI markers as MSI-H, one positive MSI marker as MSI-L, and no positive MSI markers as MSS (microsatellite stable).

Mutational analysis

Mutations for *PTEN* (exon1-8), *K-Ras* (exon1 and 2) and *PIK3CA* (exon9 and 20) were analyzed as previously described (Minaguchi *et al*., 2001; Oda *et al*., 2005, 2008).

Statistical analysis

The association of variables related to clinical characteristics was evaluated by Fisher's exact test. The *P*-values obtained in all tests were considered to be significant at $P<0.05$. Survival